Probing Crystalline Color Superconducting Phase of Quark Matter through Universal Relations for Hybrid Stars

Joshua Cole Faggert

Mentors: Prof. Kent Yagi, UVA, Shu Yan Lau, UVA

This thesis is submitted in partial completion of the requirements of the Distinguished BS Astronomy-Physics Degree

Department of Astronomy
University of Virginia
May 12, 2023

Abstract

The nature of the dense matter equation of state remains an open question, as physicists from a variety of disciplines attempt to tackle this question from different perspectives, especially via the study of neutron stars (NS). At the high densities associated with NS cores, crystalline color-superconducting (CCS) phases of quark matter could possibly occur from LOFF pairing of deconfined quarks [1]. The rigid behavior of this crystalline structure causes the tidal deformation of neutron stars to be less than fluid stars, causing deviations in the Love-C universal relations describing NS. Implementation of the rigidity of CCS phase via density-dependent shear modulus into constant sound speed models developed by [2] was conducted to investigate the deviation of these models from the universal relations. Models that agreed strongly with observational constraints on NS masses and radii showed upward of 10% fractional deviation from the best fit for the Love-C universal relation. This indicates that better measurements of the tidal Love number and compactness could enable the constraint of the parameters describing CCS equation of state, furthering our knowledge of the behavior of matter at the highest densities in the universe.

Keywords: Love-C, universal relations, hybrid stars, quark matter

1 Introduction

Neutron stars (NS) demonstrate some of the universe's extreme conditions under which the behavior of matter is not fully understood. The densities at the center of these astronomical objects are thought to get up several times nuclear density ($\approx 10^{14}\mathrm{g/cm}^3$), indicating that accurate and applicable knowledge of the strong force will be necessary in order to describe the behavior of matter in the centers of the neutron stars NSs . While the equations of state (EoS) that describe the relationship between the density and pressure are thought to be fairly well-known near the surfaces of NSs, there is a multitude of proposed equations of state to describe the NS interior. A variety of methods have been developed to create these EoS, including perturbative QCD, mean force field models, and phenomenological methods.

Equipped with an EoS, one can go on to solve the interior stellar structure of stars according to the Tolman–Oppenheimer–Volkoff (TOV) equations which describe a spherically symmetric, isotropic body in static equilibrium under a general relativistic framework, required due to the strong gravitational fields and very compact nature of NSs, second only to black holes, given by

$$\frac{dP}{dr} = -\frac{Gm}{r^2}\left(1+\frac{P}{\rho c^2}\right)\left(1+\frac{4\pi r^3 P}{mc^2}\right)\left(1-\frac{2Gm}{rc^2}\right)^{-1} \tag{1}$$

where r is the radial coordinate of the star, m is the gravitational mass contained within r, P is the pressure, ρ is the density, and G is Newton's gravitational constant. In conjunction with mass continuity, the interior structure is uniquely determined given a specific equation of state.

Given a variety of input central densities, calculations of important quantities of NS's such as radius and mass can be predicted, producing mass-radius plots that will be shown throughout this paper. As we gradually discover more NSs, whether it is through pulsar timings, supernovae, or NS binaries, more data is obtained that help constrain equations of state of stars NSs, and the behavior of matter in general at these high-density regimes. The use of NSs and the various observations we can make of them is essential, as these conditions are inaccessible to any terrestrial laboratory.

With the rise of multi-messenger astronomy, the tools and measurements available to astronomy and physics are constantly growing, enabling the study of problems from multiple perspectives.

Multi-messenger astronomy is essential to the study of NS equations of state. Electromagnetic measurements in the radio regime of pulsars in binary systems allow the measurement of the mass of NSs, which have currently provided the maximum observed NS mass of $2.14^{+0.10}_{-0.09}M_{\odot}$ [3]. X-ray observations by missions such as the Neutron Interior Composition Explorer (NICER) aim to provide constraints on the radius of NSs by measuring the time-variability of soft X-ray emission from hot spots on spinning NSs [4]. Lastly, the advent of gravitational wave observatories, most notably the Laser Interferometer Gravitational-Wave Observatory (LIGO), has enabled the measurement of NS properties by detecting the gravitational waves emitted during the merger of binary NSs systems. The combination of these different observational techniques gives data with which we can compare the theoretical predictions of NS structure by the equation of state.

The particular equation of state being considered in this study explores the feasibility of more exotic matter that may be associated with the extremely high densities of NS cores. Near or above nuclear saturation densities, the exact form or behavior of matter is unclear. Some predictions suggest that deconfined quarks may exist in these density and temperature regimes, producing color-superconducting phases of matter in this region. Knowledge of color superconducting phases indicates that it might occur in compact stars. The conditions for the transition to color-superconducting matter should arise in the NS core a short time after their formation based on transition temperature estimates/calculations [5]. One of these phases, named crystalline color-superconducting (CCS) phase, consists of these deconfined quarks that form interaction pairs similar to the BCS pairs, described more accurately by a process called LOFF pairing [1]. This predicted phase is of particular interest with the rise of gravitational wave observatories, as the solid-like structure makes the cores of these hybrid stars rigid, allowing them to resist deformation of their shape under strong tidal forces from a binary companion more strongly, a measurable quantity from the waveforms of gravitational wave-observatories.

NSs' closely related companion, black holes, exhibit fascinating universality; the external gravitational field of stationary and isolated black holes depends solely on three parameters: its mass, its spin, and its charge. These conclusions suggest that the contents that created these celestial objects do not factor into the properties of the black hole, only the contributions of the composite particles' energy, charge, and angular momentum [6]. However, astrophysical black holes accrete and interact with matter, and other massive objects such as stars, white dwarfs, and NSs have stellar surfaces and complex compositions that we expect to have a direct effect on the gravitational fields and properties of these objects. However, NSs have been shown to exhibit approximately universal relations, or relationships between properties that are roughly insensitive to the internal composition of the NS [6]. These approximate universal relations demonstrate a powerful result of general relativity, and a powerful test for studying potential deviations from these universal relations from model equations of state, where we can compare to the growing set of mass, radius, and tidal deformability measurements in order to gather more information on the behavior of matter in NSs. Before examining the deviation of NS models, the exact universal relations must be understood in more detail.

2 I-Love-Q and Love-C

One of the most well-known universal relations of NSs is the I-Love-Q relation, which provides relationships between the reduced moment-of-inertia $\bar{I}$, the tidal Love number $\bar{\lambda}$, and the quadrupole moment$\bar{Q}$ that is insensitive to a NS's EoS, discovered by Yagi and Yunes (2013) [7]. These relations have been found to be approximately universal to around 1%, showing striking universality

for physical systems. Figure 1 from Yagi and Yunes shows both the I-Love and the Q-Love relations and the large degree of uniformity to the lines of best fit. The lower plot shows the fractional error to the best fit for the models, with most EoS having lower than 1% fractional error [6]. However, it is hard to obtain simultaneous measurements of the moment of inertia of a system and the tidal Love number for the same system, making the process of taking observational constraints to test these relations on physical NSs currently difficult.

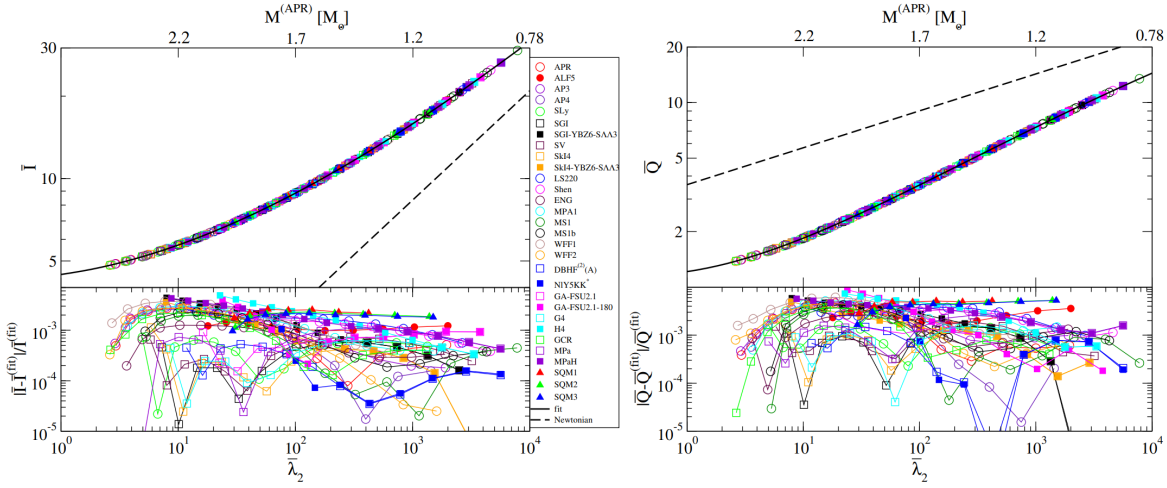

Figure 1: This figure from Yagi and Yunes (2017) [6] shows the I-Love (dimensionless moment of inertia- dimensionless tidal Love Number) and the Q-Love (quadrupole moment-dimensionless tidal Love Number) universal relations. These quantities are plotted for calculations run using a variety of EoSs as well as the fractional error of the EoSs compared to a line of best fit to these EoSs. They show show insensitivity to the 1% level.

In a similar manner to I-Love-Q, universal relations between the tidal Love number, $\bar{\lambda}$, and the compactness parameter, $C \equiv M/R$. The compactness parameter is the dimensionless ratio of M, the mass of the star, over R, the radius of the star in study. Generally, the higher compactness of an object, the more important general relativistic effects are in a calculation. The Love-C universal relation was first studied by Maselli et. al [8], where they found it to be universal to within $\sim 2\%$. Studying this relationship with a wider and more modern assay of EoSs finds that the maximum deviation for NS objects is 6.5%, and larger for quark star sequences [6]. Figure 2 from Yagi & Yunes 2017 demonstrates the universality of the Love-C relation for many EoS, several based on different principles of physics or calculation methods [6].

The Love-C relation is of particular interest to this study because it involves a property is directly affected by the existence of a rigid/crystalline core. The introduction of rigidity to the center of NSs will reduce the tidal deformation of the star in a binary pair, which causes the tidal Love number in the Love-C to shift away from the universal fit. These shifts from the universal relations line can be compared to the few systems with current measurements of Love extracted from GW observatories and compactness obtained from the NICER observatory. Ideally, with more runs of Advanced LIGO and other gravitational wave observatories, more values of tidal deformation in conjunction with compactness can be obtained for use in constraining NS equations of state.

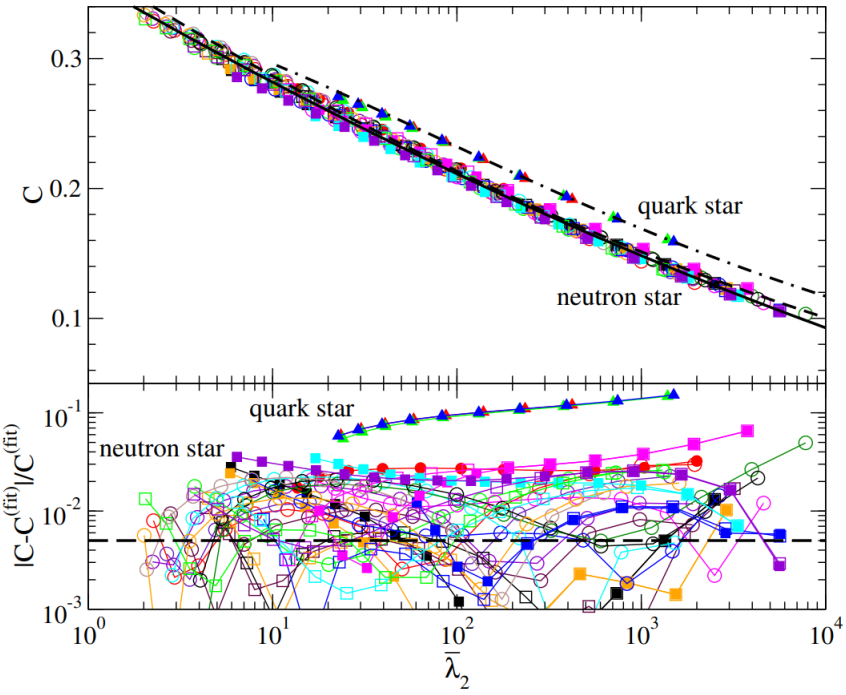

Figure 2: This figure from Yagi and Yunes (2017) [6] shows the Love-C (dimensionless tidal Love Number-compactness) universal relation. These quantities are plotted for calculations run using a variety of EoSs as well as the fractional error of the EoSs compared to a line of best fit to these EoSs. They show show insensitivity to the 10% level

3 Relativistic Calculation of Tidal Deformability of Hybrid Stars

Once equipped with an EoS, the TOV equation can be solved numerically to yield the stellar structure, giving properties such as mass, radius, and compactness, giving initial conditions such as central density. The solid properties of the solid star are considered only at the perturbative level, while the background solution is solved as a perfect fluid. Once this static/perfect fluid is solved for the static case, the tidal deformation of the NS is considered perturbatively by using the linearization of Einstein's equations in conjunction with the conservation equation that is associated with the matter field of the NS, represented by equations (2) & (3) . This section follows the formulation by Lau et. al 2019, the author of the numerical code being used [9].

$$\delta G_{\alpha\beta} = 8\pi\delta T_{\alpha\beta} \tag{2}$$

$$\delta(\nabla^{\alpha} T_{\alpha\beta}) = 0 \tag{3}$$

The effects of NS elasticity comes into play when considering the shear portion $T^{shear}_{\alpha\beta}$ of the full stress-energy tensor. In contrast, the bulk part $T^{bulk}_{\alpha\beta}$ takes the perfect fluid form, used to acquire the background TOV solution. The shear portion of the stress-energy can be shown only to contribute perturbatively and not to the overall TOV structure. The perturbation to the shear portion of the stress-energy tensor follows a Hooke's Law-like relationship with the shear modulus μ and the shear strain tensor perturbation $\delta\Sigma_{\alpha\beta}$ given by:

$$\delta T^{shear}_{\alpha\beta} = -2\mu\delta\Sigma_{\alpha\beta} \tag{4}$$

Using a relationship that describes a differential equation for the shear stress tensor, a series of differential equations in terms of solid perturbation variables (a set of variables that describes the unknowns of the solid core perturbation calculation) can be obtained. Combined with a series of algebraic relationships, the relationships form a complete set of equations. By choosing regular solutions at the center of the NSs, and applying the appropriate boundary conditions at the stellar surface and the interface between the two layers of the NS, these equations for the perturbation method can be solved.

Equipped with the metric perturbation, the tidal Love number can be calculated. The metric for a static, spherically symmetric stellar model under a static external tidal field in the far field limit is first written by Thorne [10] is given by:

$$-\frac{1+g_{tt}}{2} = -\frac{M}{r} - 3\frac{Q_{ij}}{2r^3}(\frac{x^i x^j}{r^2} - \frac{1}{3}\delta^{ij}) + \frac{1}{2}\mathcal{E}_{ij}x^i x^j \tag{5}$$

where Q_{ij} is the quadrupole moment and $\mathcal{E}_{ij}$ is the external tidal field, caused by the binary partner. Q_{ij} and $\mathcal{E}_{ij}$ are related by:

$$Q_{ij} = -\frac{2}{3}k_2 R^5 \mathcal{E}_{ij} \tag{6}$$

Coupling these two equations with the perturbation solutions, the dimensionless tidal love number, $\bar{\lambda}$, can be obtained

$$\bar{\lambda} = -\frac{2}{3}k_2\left(\frac{R}{M}\right)^5 \tag{7}$$

Lau et. al (2019) describes their formulation for the calculation of the tidal Love number for the stars containing a solid quark core and a fluid outer layer, upon which this section was based, where an equation for the Love number k_2 was used to calculate the Love number for the existing scenarios.

The tidal deformability and NS structure code developed by Shu Yan Lau was used to carry out these calculations, which could be conducted for both hybrid and fully fluid stars, i.e. either containing an entire fluid star or a two-layered (outer layer fluid-inner core solid) star. This code proceeds to first generate an equation of state, based on either a model of the changing parameters or pre-existing equation of state, which is used to calculate the background solution to the TOV equation for the NS at a chosen central density. Then, the code proceeds to solve the boundary problem via the Lau et al. (2019) formalism to calculate tidal deformability for situations both including for hybrid stars with a solid core. The calculation of the Love number of a fluid star follows a prior formulation by Hinderer (2008)[11]. The code of Shu Yan Lau was modified in order to handle the CSS hybrid star model while incorporating shear modulus through a density dependent, described in Section 6.

4 Relativistic Tidal Deformability in Fluid NSs

The first calculations performed were that of entirely fluid NSs using various nuclear matter equations of state developed to explore the behavior of the interiors of NSs without introducing intricacies such as various quark matter interiors or color superconducting states for the interiors.

The main purposes of these calculations were to use these results as a comparison when we consider hybrid stars with an outer layer of nuclear matter and the core of the CCS phase.

There are a variety of equations of state that have been proposed to describe the interiors of NSs. One of the particular interests of the Love-C and stricter universal relations is the multitude of different equations of state that exhibit different mass-radius predictions which still adhere closely to these universal relations. Three different nuclear matter EoS were used in both the fluid and hybrid star calculations throughout the study. The NL3 model, a relativistic mean field model, is a stiffer equation of state [12]. Stiffness in equations of state means the pressure raises faster as a function of increasing mass/energy density, indicating that more massive NSs can be supported from gravitational collapse by internal pressure. This particular equation of state was used in Alford and Han's paper about the general stability of hybrid stars [2]. Akmal, Pandharipande, and Ravenhall (APR) is a more relaxed equation of state compared to NL3 and is constructed via a variational summation method including multiple nucleon interactions[13]. SLy4 equation of state model for the nuclear matter was also commonly used in the fluid and hybrid star calculations, which is a non-relativistic, mean-field nucleon-nucleon interaction-based model [14].

Each of these equations of state only considers fully fluid NSs. With the EoS input, we can calculate the masses and radii of the NSs with varying central densities. Plotting the NS mass vs. the radius produces Mass-Radius (MR) relations, which are highly dependent upon the equation of state, as can be seen in Figure 3.

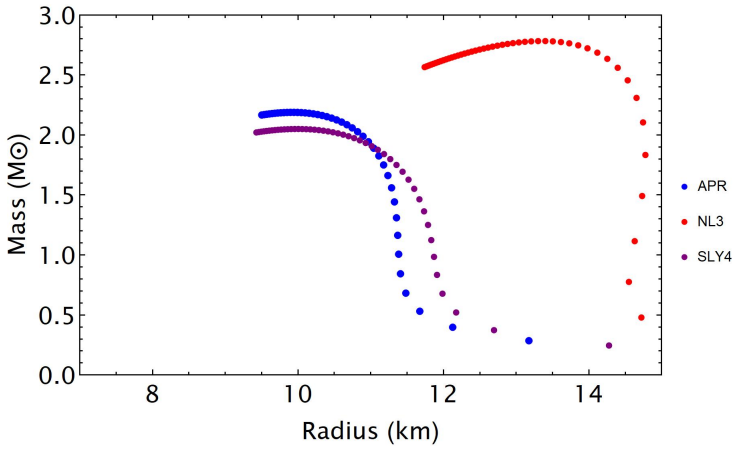

Figure 3: MR curves for the fluid NL3, APR, SLY4 equations of State

The maximum mass of NL3 reaches is approximately 2.8 $M_\odot$, demonstrating the stiffness of this EoS as compared to the SLy4 and APR, which have maximum mass's of $\sim 2.0 M_\odot$ and $\sim 2.2 M_\odot$.

A key part of this investigation focused on the calculation of the tidal deformability of the various stars constructed in the code, for both fluid and hybrid stars. Large deviations from the Love-C relations are most interesting, as better measurements will hopefully allow us to more tightly constrain EoS's that don't agree with observations. The Love-C relation of these three equations of state are plotted in 4 along with a fit from Yagi and Yunes [6] that incorporated a variety of equations of state based on differing physical principles & methods.

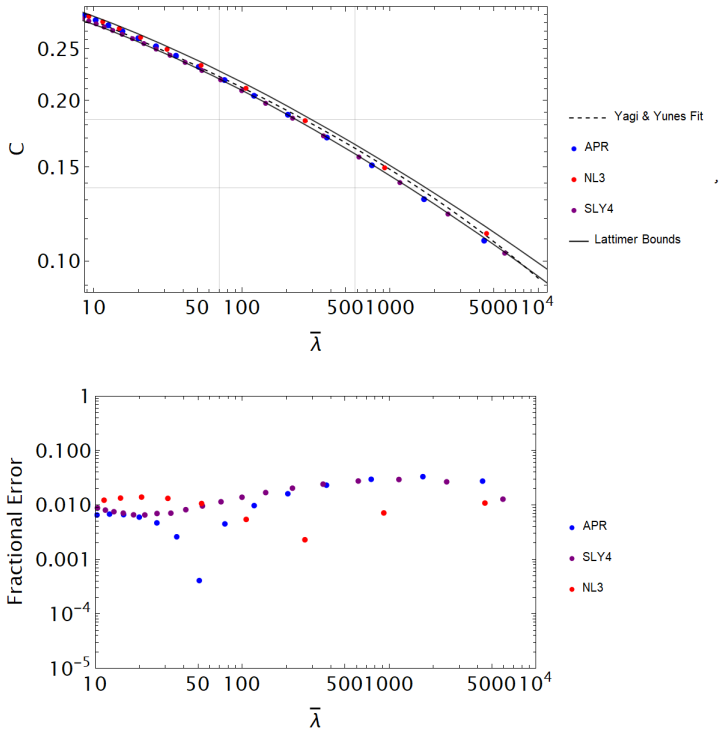

Figure 4: (Top) This shows the dimensionless tidal deformability vs. the stellar compactness of three separate nuclear matter equations of state along with a fit to the universal relation by Yagi and Yunes. The solid lines represent the top and bottom bounds of equations of states in the Love-C relations from [15], which are used throughout the study as a representative spread in EoS in the Love-C relations (Bottom) This figure shows the fractional error in the compactness with respect to the best fit line from [6]

From the Love-C plots, we can see how these highly variable equations of state in terms of the mass-radius relationship agree strongly with the universal relations, with all of the fractional errors below 5% deviations for a large range of tidal deformabilities. The lower plot of Figure 4 shows the fractional difference of the calculated tidal deformability $\bar{\lambda}$ from the best fit calculated from many different EoS from Yagi & Yunes (2017). We expect to see larger deviations from this Love-C relation when we include crystalline NS cores in the calculations. These deviations are studied through two different models, discussed below.

5 Crystalline Color Superconducting (CCS) Phase Hybrid Stars - MIT Bag Model

The first method by which this CCS phase was incorporated into the model of hybrid stars was using an equation of state based on an MIT Bag Model to describe the CCS phase, the shear modulus of which was dependent primarily upon the gap parameter associated with the pairing that creates the CCS phase [16].

The process that creates this novel state of quark matter is called LOFF pairing, first considered by Larkin, Ovchinnikov, Fulde, and Ferrrel [1],[17]. This LOFF pairing is analogous to BCS pairing that describes electron pairing in superconductors. However, the key difference between these mechanisms is that LOFF pairing allows Cooper pairs with non-zero total momentum. These

pairs, with different Fermi surfaces, can come together and interact if their Fermi momenta are sufficiently close together, lowering their overall energy through an attractive interaction. In the context of the NSs, this involves the propsect of pairing between deconfined quarks in the very high-density regions of the NS cores [5].

When two fermions experience an attractive interaction and their Fermi momenta are the same, they pair in a BCS manner. This idealization is not likely to be as applicable to NSs, because it is unlikely that the up, down, and strange quarks within the core will have the exact same Fermi momentum, a requirement for this type of pairing. If the Fermi momenta of the different quarks are very different, a chemical potential dependent quantity, no pairing is expected. But, in the intermediate range between no and large differences in Fermi momenta lies the possibility of LOFF pairing. For some range of differences in chemical potential, a condensate of pairs with momentum $\mathbf{q}+\mathbf{p}$ and $\mathbf{q}-\mathbf{p}$ is favored over BCS pairing or no pairing[5]. In position space, the LOFF quark pairs will tend to vary in space like $\Sigma_a e^{2iq^a\cdot x}$. This indicates that the momentum represents the reciprocal vectors which can be shown to define the crystalline structure of condensate[18]. The crystalline structure formed by the pairing of this condensate causes the NS core to act as a solid and has rigidity, the shear modulus of which was originally calculated by Mannarelli et. al [18]. A more rigid core will deform less from gravitational tidal forces, like in a binary, decreasing its tidal deformability, having an impact on the Love-C relation of a NS that contains this sort of phase.

A phenomenological equation of state that approximates the behavior of the quark matter predicted in the center of neutron stars was developed [16]. This quark matter equation of state consists of a power series expansion in the quark chemical potential μ. The equation of state is given in equation (8).

$$\Omega_{QM} = -\frac{3}{4\pi^2}a_4\mu^4 + \frac{3}{4\pi^2}a_2\mu^2 + B_{\text{eff}} \tag{8}$$

Because the CCS phase acts as a solid and exhibits rigidity, it has a non-zero shear modulus. This shear modulus will affect the amount that the core is tidally deformed and thus will affect the Love number calculated for the specific hybrid stars that follow this equation of state. QCD and related calculations pertaining to CCS phase and its rigidity give the resulting expression for the shear modulus of the CCS phase[18], given in equation 9.

$$\nu_{QM} = 2.47\text{MeV/fm}^2\left(\frac{\Delta}{10\text{MeV}}\right)^2\left(\frac{\mu}{400\text{MeV}}\right)^2 \tag{9}$$

The parameters of the MIT Bag Model application to the CCS phase in hybrid stars are a_2, a_4, B_{eff}, Δ or the gap parameter associated with the CCS pairing, and the transition pressure p_{trans}. As suggested by Mannarelli, the gap parameter is likely restricted between 5 and 25 MeV. The gap parameter does not show up directly in the parameterized equation of state, but it does affect the rigidity of the CCS core and thus will make the core more rigid the higher the gap parameter chosen. In these calculations, a gap parameter of 25 MeV was primarily chosen unless stated otherwise. For the parameter a_4, which parameterizes the QCD corrections to the pressure of a free-quark Fermi sea, we set a value at 0.85 unless otherwise stated, which was in the range of reasonable values for this correction parameter that obtains heavy hybrid stars. A a_4 value of 1.0 corresponds to 3 non-interacting quarks, values less than this account for QCD corrections and quark interactions. The Bag Constant associated with the EoS was set at 160^4. a_2 was set to 10^4 for most trials. The main parameter changed was that of the transition pressure, or the pressure at which the equation of state turned from nuclear matter to CCS quark phase.

By varying parameters such as the transition pressure and the gap parameter, two of which expected to have an effect on the measurements of tidal deformability, we could further understand parameters that describe larger deviations from the Love-C universal relation. Figure 5 explores the effect of changing transition pressure on the MR curve. The higher the transition pressure, the larger the pressure must be before the phase transition between nuclear matter and quark CCS matter occurs, meaning a smaller percentage of the hybrid star is made up of quark matter and the hybrid star more closely resembles the fluid matter equation of state. The SLy4 fluid star was more massive than these three hybrid stars, and thus the highest transition pressure hybrid star had the largest MR curve, resembling most the nuclear matter equation of state.

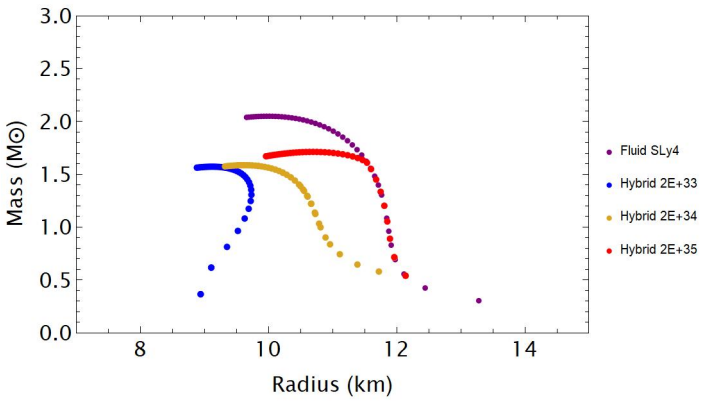

Figure 5: Mass vs. radius relation for hybrid star with the SLY4 nuclear matter EoS with changing transition pressures.

The corresponding Love-C relations of these same stars calculated for multiple central densities are shown in Figure 6. Like expected, the hybrid stars with lower transition pressure exhibit larger "solid" cores that are less affected by tidal deformation, and thus stray further from the universal relation that other equations of state follow.

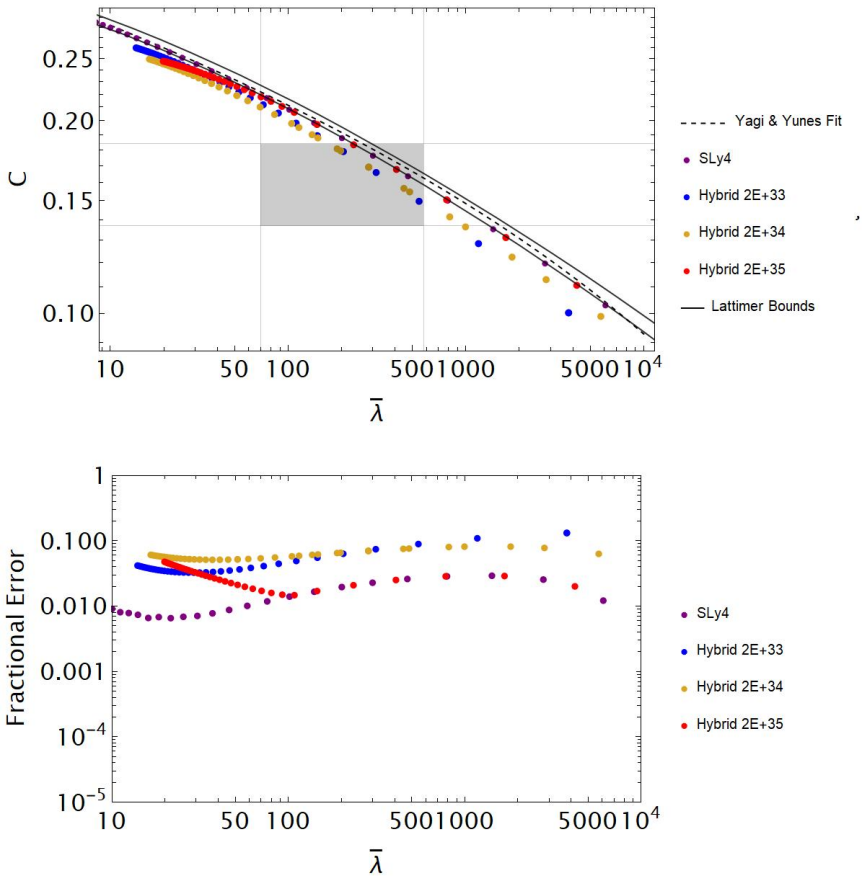

Figure 6: (Top) Love-C relation and fractional error plots for hybrid Star with the SLy4 nuclear matter EoS with changing transition pressures, all with a gap parameter of 25 MeV. The shaded region indicates the bounds of the tidal Love number and compactness values determined from the NICER & LIGO measurements of GW170817 [19],[20]. These measurement bounds are used throughout this paper. (Bottom) The fractional error in compactness as compared to the best fit is plotted vs. the tidal deformability.

These high gap parameter models show significant deviation from the Love-C relation, with some of the tidal deformability having fractional errors upper of 10%. However, these still fall in the large bounds of the LIGO measurements of GW170817 of Love and C of Figure 6. As measurement error decreases in the future, this shaded region will likely decrease in area, providing a stronger constraint on the viability of deviation from Love-C and the viability of large-deviation CCS models.

Besides transition pressure, the gap parameter describing the LOFF pairing of the CCS state was also changed. As the gap parameter does not directly factor into the equation of state (8), it was expected that altering the gap parameter would not affect the MR curve, which was confirmed in Figure 7.

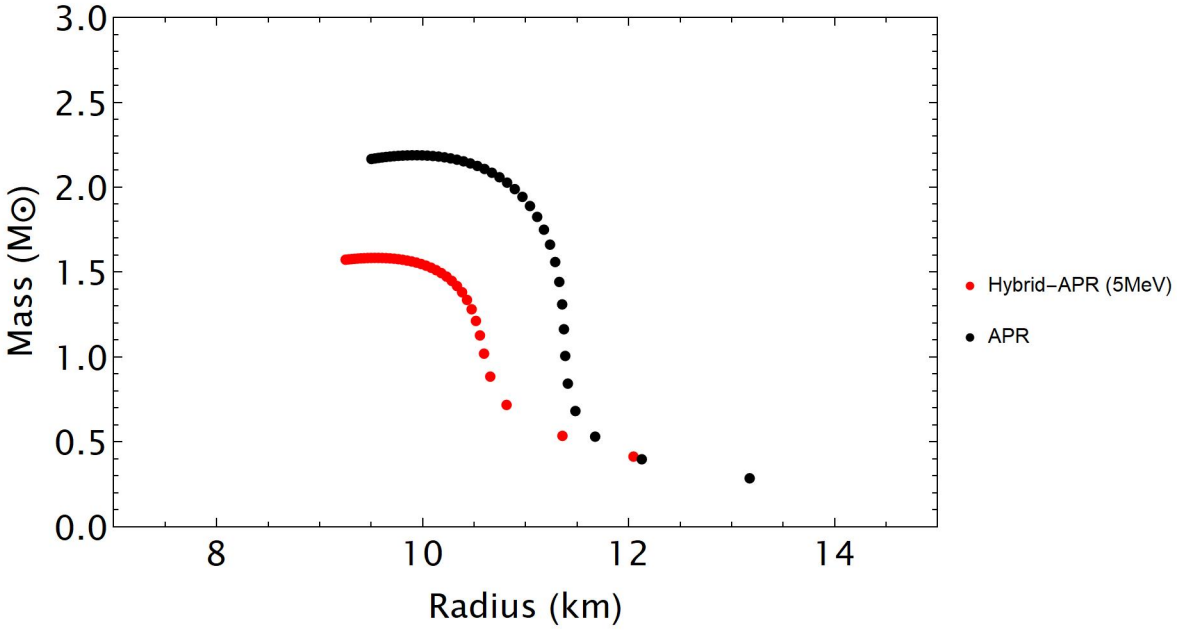

Figure 7: Mass vs. Radius relation for Hybrid Star with the APR nuclear matter EoS with changed gap parameter and the fluid star comparison. Because gap parameter does not directly affect the EoS, varying gap parameter will have the same MR relation.

However, equation 9 shows how the shear modulus of the CCS core changes with changing gap parameter from [18]. Increasing the gap parameter within the suggested constraints increases the deviation from the universal relation of the Love-C relation, as the CCS phase core exhibits more rigidity, lowering its tidal deformability for a given NS compactness. Models for hybrid star and tidal deformability using the MIT Bag Model EoS was tested with gap parameters of 5, 15, and 25 MeV.

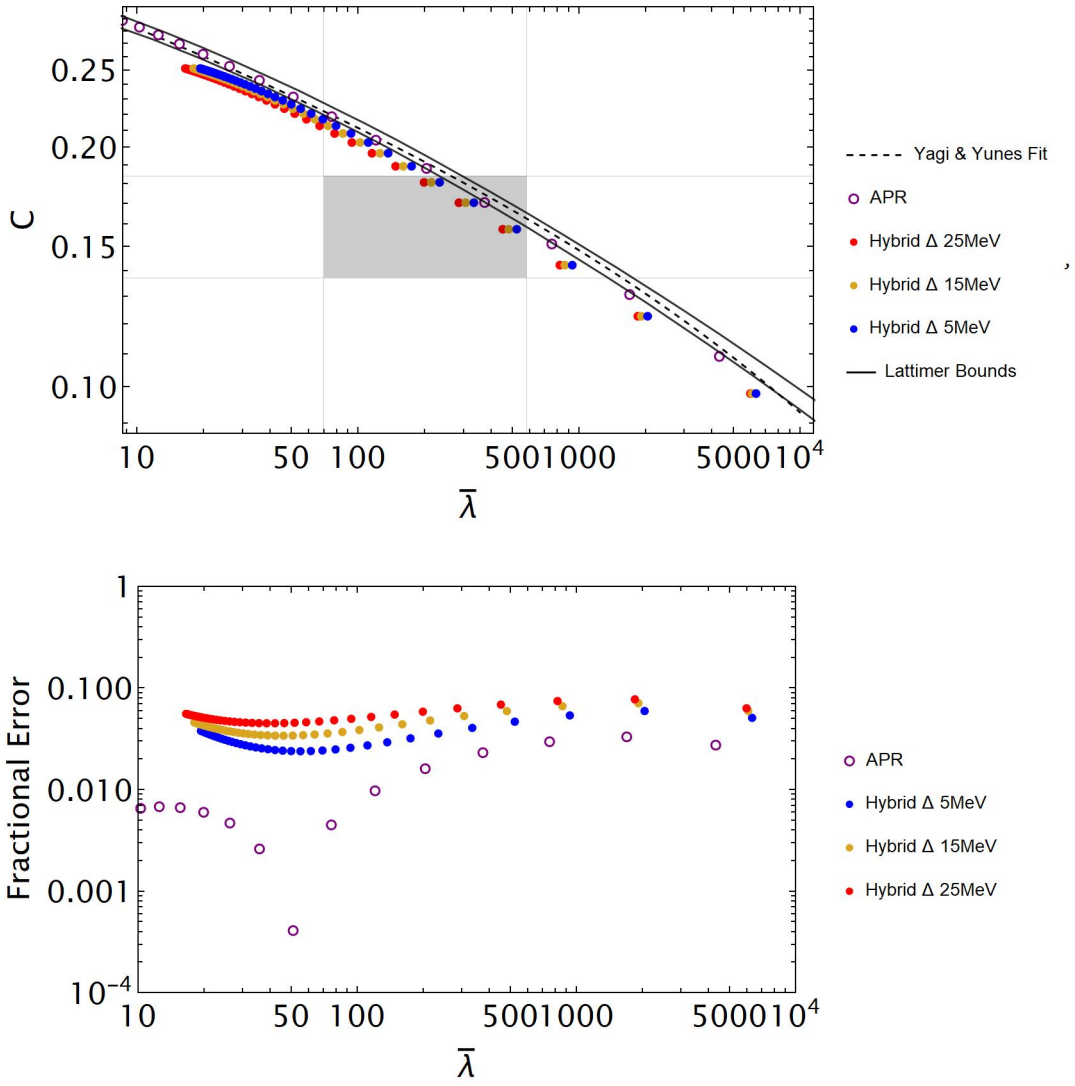

Figure 8: (TOP) Love-C relation for hybrid stars with changing gap parameter Δ including fractional error from the best-fit plot from Yagi & Yunes. (Bottom) The fractional error in compactness as compared to the best fit is plotted vs. the tidal deformability

The increased gap parameter followed the expected pattern and showed that deviations nearing 10 % could be achieved for the higher end of likely values for the gap parameter of LOFF pairing by Mannarelli.[18]. Describing the CCS phase by the MIT Bag Model in conjunction with calculations of CCS quark phase rigidity takes a microscopic physics approach to predict NS properties. We will explore in the next section a different approach that seeks to generally describe hybrid stars from a more macroscopic approach.

6 Crystalline Color Superconducting (CCS) Phase Hybrid Stars - Constant Sound Speed Model (CSS)

Where the previous model was motivated by applying an MIT Bag Model to describe the behavior of quarks in the center of the cores in order to provide a phenomenological equation of the neutron core, this section's model mimicked previous models [2] that assume a constant sound speed in

the quark NS core, motivating an equation of state that is built around this assumption. A density-dependent shear modulus was included into this CSS equation to incorporate the effects of rigidity.

The independence of sound speed w.r.t. density, is a reasonable simplification to apply to the quark matter equation of state. There are Nambu-Jona-Lasiono models of the CCS phase equation of state that match this density independence very well. Perturbative quark matter results show rough density independence and sound speeds [21]. Having a constant sound speed as a parameter allows the modification of the stiffness of our equation of state, which as we'll see, increases the maximum mass of our hybrid star. This model also assumes a first-order phase transition between the nuclear matter equation of state, which will be varied throughout the investigations, which describes the matter prior to the transition, and the quark matter constant sound speed model which describes matter past the transition pressure.

The Eos describing the hybrid star is represented by:

$$\varepsilon(p) = \varepsilon_{NM}(p) \qquad (p < p_{trans}) \tag{10}$$

$$\varepsilon(p) = \varepsilon_{NM}(p_{trans}) + \Delta\varepsilon + c_{QM}^{-2}(p - p_{trans}) \qquad (p > p_{trans}) \tag{11}$$

The model, equation (11) from [2] is parameterized by four important parameters: c_{QM}^2, p_{trans}, $\Delta\varepsilon$, and ε_{NM}, where ε represents the energy density, which is related to ρ by $\varepsilon = \rho c^2$. c_{QM}^2 describes the sound speed within the quark matter core, which quantifies how the matter responds to increasing density with an increase in pressure. The larger the sound speed, the stiffer the equation of state and the more massive the hybrid star as a result. p_{trans} represents the pressure at which the first-order transition between nuclear/hadronic matter and quark/CCS matter occurs. Larger transition pressure indicates that the transition between phases occurs further into the NS, meaning a smaller portion of the NS is composed of quark matter. $\Delta\varepsilon$ describes the energy density gap at the first-order transition between the starting energy density of the quark matter and the last energy density of the hadronic matter.

While the rigidity of the CCS phase was taken through Mannarelli's calculation of the shear modulus based on the gap parameter in the previous hybrid star model, there needed to be a new way to express the rigidity of the CCS phase solid core in our constant sound speed formulation. As a solution to this issue, we used the MIT Bag Model type formulation in conjunction with Mannarelli's calculation of the rigidity to motivate a density-dependent shear modulus. Using (8),the number density, n, can be calculated with thermodynamic relations between the grand thermodynamic potential and the chemical potential.

$$n = -\frac{1}{3}\frac{\partial\Omega}{\partial\mu} = \frac{1}{\pi^2}a_4\mu^3 - \frac{1}{2\pi^2}a_2\mu \tag{12}$$

With the number, the energy density of the MIT Bag Model for the quark matter can be calculated:

$$\varepsilon = \Omega + 3\mu n == \frac{9}{4\pi^2}a_4\mu^4 - \frac{3}{4\pi^2}a_2\mu^2 + B_{eff} \tag{13}$$

Using (13), We can solve for the chemical potential fully in terms of the density (related to energy density by $\varepsilon = \rho c^2$) and the parameters of the MIT Bag Model. This is shown in equation 14, setting $c \equiv 1$.

$$\mu^2 = \frac{1}{6a_4}\left(a_2 + a_2\sqrt{1 + \frac{1}{a_2^2}16\pi^2 a_4 \frac{\rho_{qm}}{\frac{e^4}{\hbar^3}}} - B_{\text{eff}}\right) \tag{14}$$

Using the shear modulus form of equation (9), we can obtain an expression (equation (**??**)) for the shear modulus of the MIT model to motivate incorporating rigidity into the CSS mode.

$$\nu_{QM} = 2.47\text{MeV/fm}^2\left(\frac{\Delta}{10\text{MeV}}\right)^2\left(\frac{1}{400\text{MeV}}\right)^2\frac{1}{6a_4}\left(a_2 + a_2\sqrt{1 + \frac{1}{a_2^2}16\pi^2 a_4 \frac{\rho_{qm}}{\frac{e^4}{\hbar^3}}} - B_{\text{eff}}\right) \tag{15}$$

At high densities, this equation goes as the square root of density, where we can ignore the constant term that contains the parameter a_2. Since we are modeling the core as the quark matter with this rigidity, a model was chosen to have a constant factor multiplied by the square root of density to represent the shear modulus of the CCS phase. The inclusion of the rigidity of the form (16) into CSS allows the description of solid core quark matter via the CSS model. Figure 9 shows the adherence of the model with $\kappa = 7 \times 10^{26}$ cm$^{1/2}$ g$^{1/2}$ s^{-2} (16) to CCS rigidity as a function of density (9):

$$\nu_{QM} = \kappa\sqrt{\rho_{qm}} \tag{16}$$

The value of κ was calculated from nominal values typical values that describe the MIT Bag Model suggested by Alford [16], although this parameter is free to change.

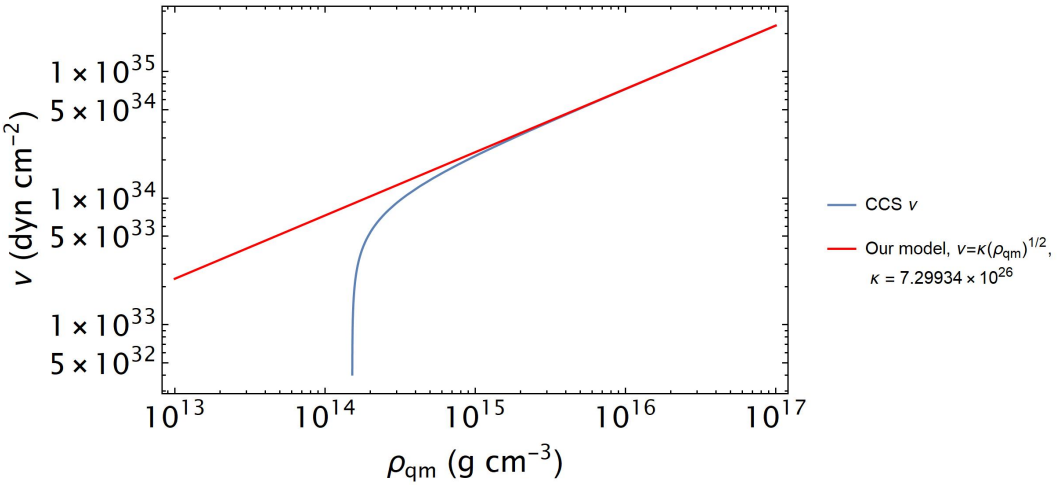

Figure 9: CSS shear modulus model vs. calculation of shear modulus from Mannarelli as a function of density

We first explore how the MR curves and Love-C relations change with changes with parameters, proceeding to investigate large deviations in models that agree with current observational constraints on the masses and radii of NSs.

6.1 Exploring the Changing Parameters of the Hybrid Star

We first examine the effects of changing the various values that parameterize the constant sound speed model for the CSS hybrid stars.

6.1.1 Changing Sound Speed

The sound speed is the main parameter that controls the stiffness of the equation of state describing the CCS core. Our upper limit for the sound speed is that of the causal limit, which corresponds to c_s^2 equal to the speed of light squared. There is no firm lower limit on the sound speed of the quark matter in these environments, but it is thought that $c_s^2 = \frac{1}{3}$ is associated with weakly interacting quark matter [2], which was often used as the lower bound on the sound speed in exploring these models, especially those that have nuclear matter EoSs that are stiffer.

The sound speed of the hybrid star EoS, using an APR nuclear matter envelope and a set pressure and energy gap, was changed to investigate its effect on the MR curves and Love-C relation. The energy gap for each of these models was chosen to be 5×10^{12} g cm^{-3}. The sound speed was changed varied from $c_s^2 = \frac{1}{3}$ to 1 (where sound speed is measured as a fraction of the speed of light) at several steps, and these calculations were conducted at three different transitions pressures.

The nominal transition pressure for many of the models throughout this paper is $2{\times}10^{34}$ dyn cm^{-2}. The MR curves for changing sound speeds at this pressure are shown in Figure 10. We can see that as the sound speed increases, the hybrid star equation of state becomes more and more stiff. This permits large masses of hybrid stars, because each central density can obtain a higher pressure to resist against gravity forces. The EoSs of the several hybrid stars follow solely the APR EoS until the central density becomes high enough for quark matter to appear in the core, where it begins to deviate from this relationship. For realistic models of the EoS, we need the MR curves to reproduce the mass of the highest record NS mass, shown with uncertainties by the band in this 10.

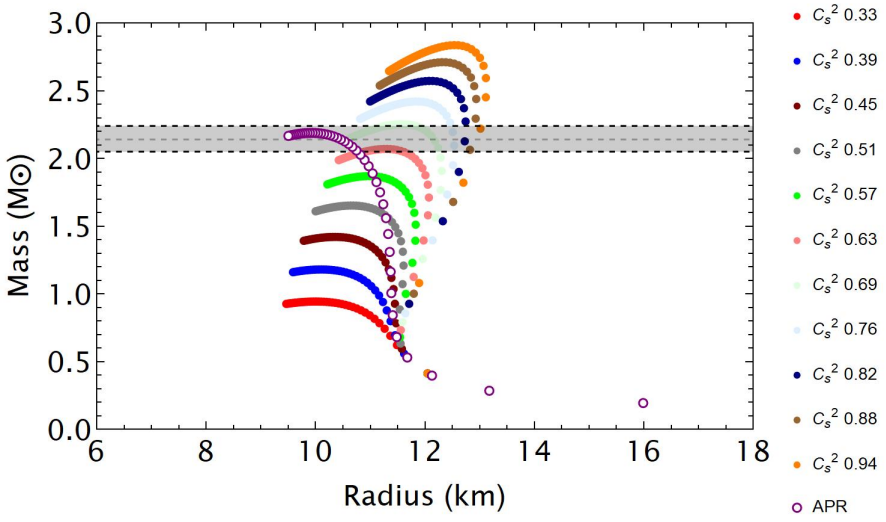

Figure 10: Mass vs. radius relation for hybrid star with the APR nuclear matter EoS with changing sound speed, all with the transition pressure of 2×10^{34} dyn cm^{-2}

Examining the Love-C relations of these NSs, we see that they tend to deviate more strongly at higher central densities and higher compactness (moving toward the left in Figure 11). Increasing the sound speed of the quark matter tends to push this relation toward smaller tidal deformations and larger compactnesses for the same value of the NS central density.

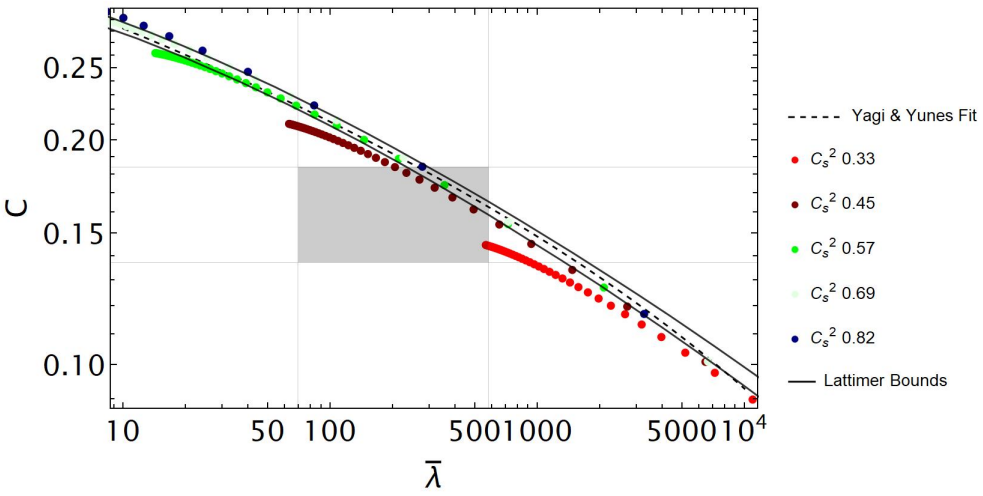

Figure 11: Love-C relations for Hybrid Star with the APR nuclear matter EoS with changing sound speed, all with the transition pressure 2×10^{34} dyn cm^{-2}

Increasing the transition pressure to the 2×10^{35} dyn cm^{-2}, we see the same trend in the MR relations. Increasing the sound speed of the quark core of the NS increased the stiffness of the overall NS, allowing the possibility of larger masses. Because the pressure at which the NS transitions from nuclear matter to quark matter is higher than the previous set of models, the overall fraction of the hybrid star that is made up of the CCS quark matter is smaller than in the previous models. This means that the MR curves of the hybrid star models follow the MR curve of fluid APR EoS much more closely, only breaking off from this trend when the pressure gets high enough, which is easier to obtain at the larger values of central density. This behavior can be seen in Figure 13.

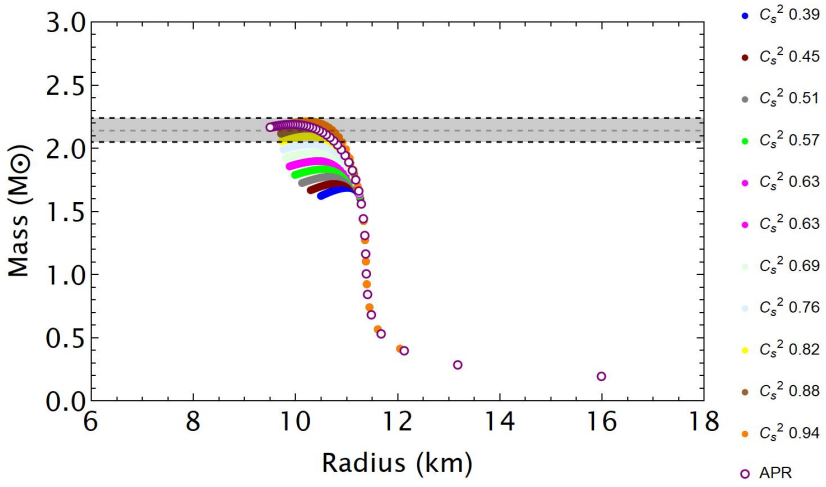

Figure 12: Mass vs. radius relation for hybrid star with the APR nuclear matter EoS with changing sound speed, all with the transition pressure 2×10^{35} dyn cm^{-2}.

On account of the hybrid star being made of less quark matter due to the high pressure for transition, the Love-C relation of the hybrid star will also follow the APR Love-C relation very closely. This corresponds to strong agreement with the universal relation. The shift to higher

compactnesses and lower Love number with increasing sound speed was also observed in these models in Figure 12.

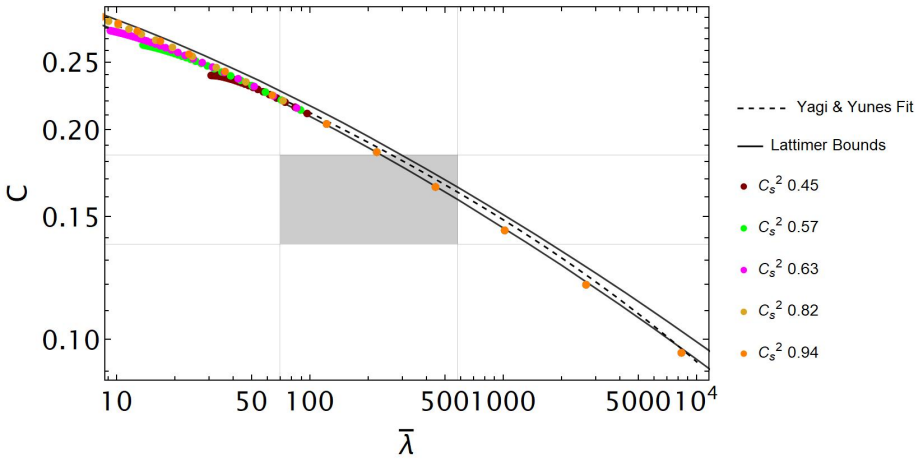

Figure 13: Love-C relations for hybrid star with the APR nuclear matter EoS with changing sound speed, all with the transition pressure 2×10^{35} dyn cm^{-2}.

Examining the effects of changing sound speed at a much lower transition pressure shows similar trends with interesting results in the stellar structure. At 2×10^{35} dyn cm^{-2}, a larger fraction of the hybrid star is composed of quark matter, especially at the highest central densities. Due to this, there is a much larger effect on the MR curves in increasing the mass of the hybrid star with increasing sound speed. The highest sound speeds represent very stiff equations of state (likely not very realistic) with hybrid stars reaching upward of $3M_{\odot}$. Additionally, increasing the sound speed gradually pushed the radii of these stars outward, showing MR curves that resemble full quark stars more closely. These MR curves are shown in 14. The shift of the Love-C relation to higher compactness and lower tidal Love number is seen at this transition pressure as well 15, giving a good idea of the impact of changing sound speeds.

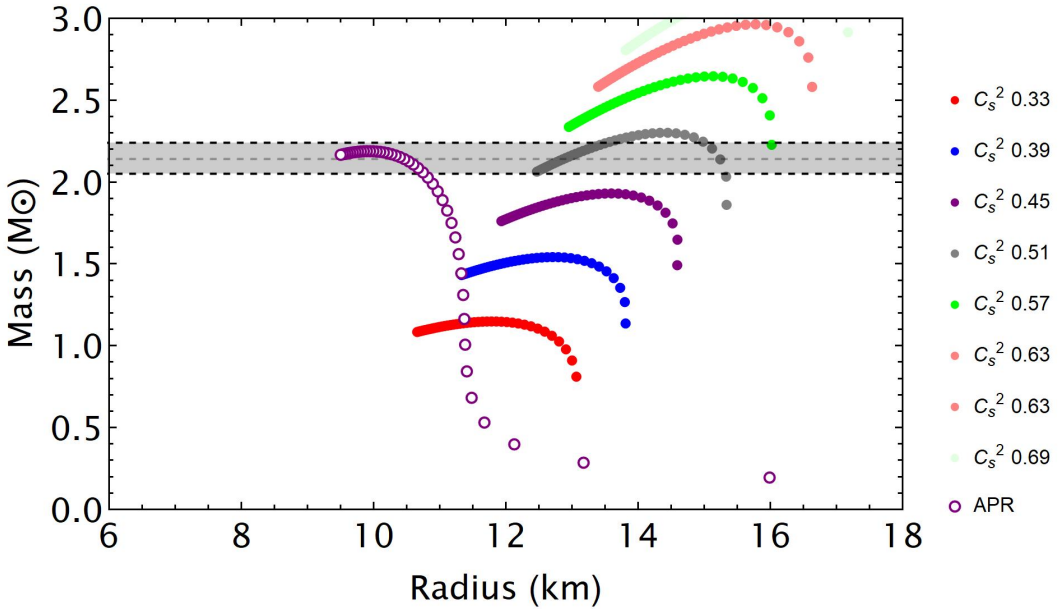

Figure 14: Mass vs. radius relation for hybrid star with the APR nuclear matter EoS with changing sound speed, all with the transition pressure 2×10^{33} dyn cm^{-2}.

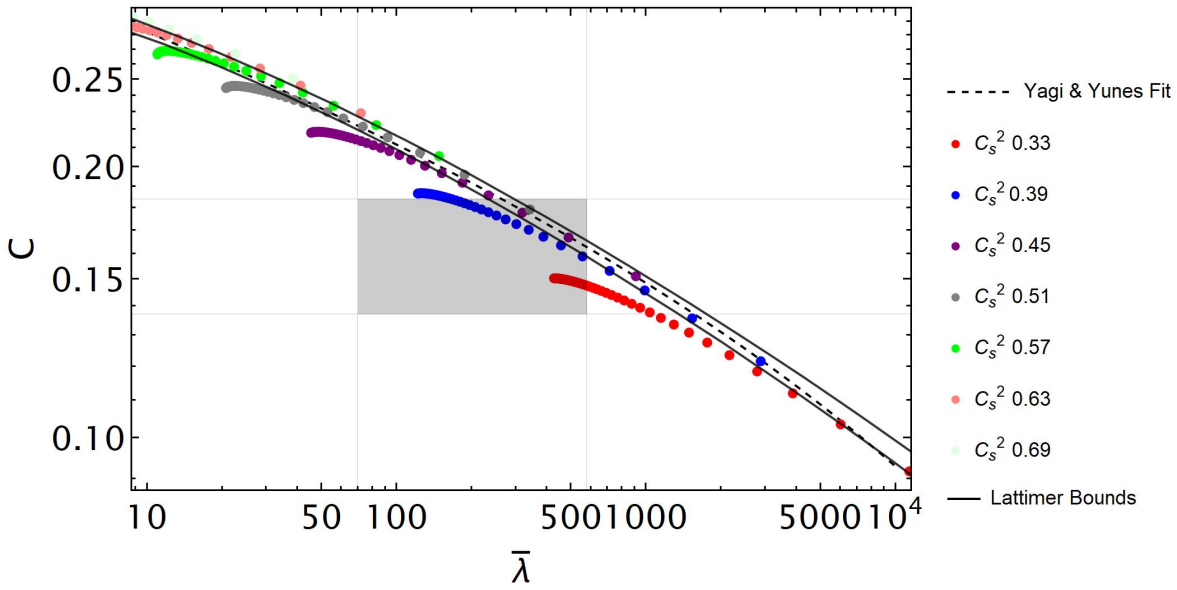

Figure 15: Love-C relations for hybrid star with the APR nuclear matter EoS with changing sound speed, all with the transition pressure 2×10^{33} dyn cm^{-2}.

6.1.2 Changing Energy Gap at Transition

The parameter energy gap $\Delta\varepsilon$ describes the jump in energy density at the phase transition between the nuclear matter equation of state and the quark matter equation of state described by (11). The starting ε for the quark matter portion of the hybrid star, seen in (11), is the combination of the energy density of the nuclear matter EoS at the set transition pressure plus this parameter

$\Delta\varepsilon$. This formulation allows for the first-order nature of this transition, which is shown to having interesting effects on the stellar structure and Love-C relations of the hybrid stars involving them.

The lowest value for $\Delta\varepsilon$ of $5 \times 10^{12}\,\mathrm{g\,cm^{-3}}$, like in the previous subsection. This was found to be about 1% of the energy density at a pressure of 2×10^{34} dyn cm^{-2} , the nominal transition pressure used in a majority of the models, as quoted from the APR EoS table. This value is small compared to total energy density at the transition, indicating that the effects of the energy gap will likely be small. This energy gap is increased logarithmically up to about 1000% of the energy density of the nuclear matter at the transition. Stated otherwise, the energy density gap is 10$\times$ the energy density of the nuclear matter at the transition point. This energy gap shows significant effects on both the MR curves and the Love-C relations, as discussed below.

In the same manner as the previous section, the parameter, $\Delta\varepsilon$, was varied at three separate values of transition pressure. The models with transition pressure of 2×10^{34} dyn cm^{-2} showed significant change in structure with increasing $\Delta\varepsilon$. As this gap increased, the MR curves were shifted toward smaller masses and smaller radii, creating flatter MR curves the larger this value was increased. At extreme values, the hybrid star models don't significantly increase in mass at all with increasing central density. The hybrid stars with these parameters produced smaller stars than the fluid APR EoS as can be seen in 16.

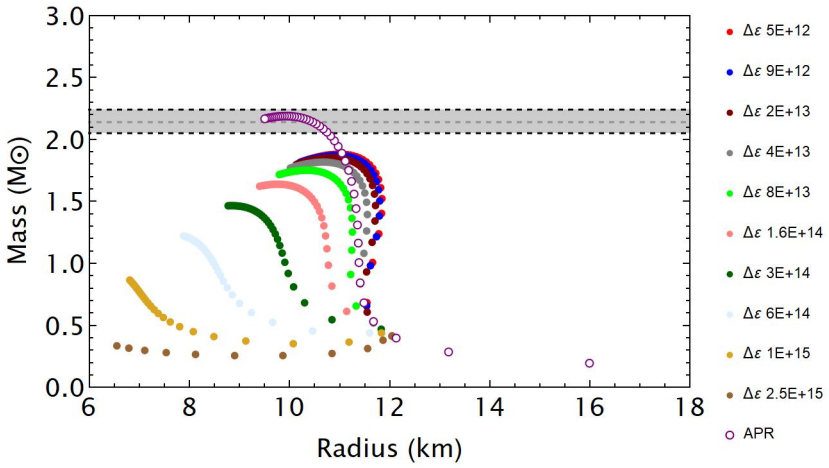

Figure 16: Mass vs. radius relation for hybrid star with the APR nuclear matter EoS with changing energy gap, all with the transition pressure 2×10^{34} dyn cm^{-2}.

When examining the Love-C relations of these hybrid stars with changing $\Delta\varepsilon$, the effects of the energy gap can be seen clearly in Figure 17. As the gap increased, the hybrid stars tended to deviate more from the best fit for the Love-C universal relation, shifting to smaller tidal deformation and lower compactness for the same values of central density.

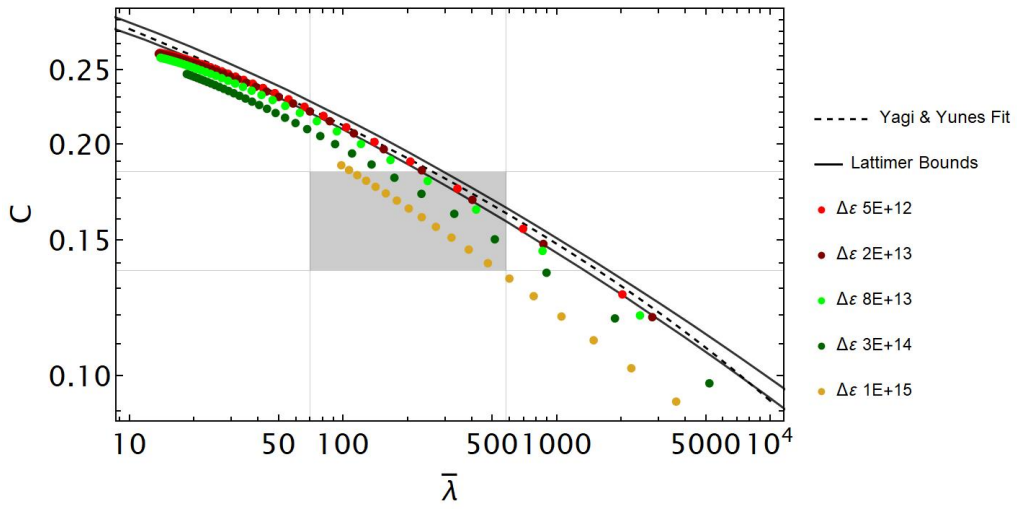

Figure 17: Love-C relations for hybrid star with the APR nuclear matter EoS with changing energy gap, all with the transition pressure 2×10^{34} dyn cm^{-2}.

Increasing the transition pressure to 2×10^{35} dyn cm^{-2}, we reexamine the effects of the gap parameter on the MR and Love-C relations. As expected, these models follow the behavior of the fluid APR NS up to higher central densities to the higher pressure required for transition to quark matter. The higher energy gaps causes the slope of the MR curves to flatten, and even reach the point where the mass decreases with increasing central density. In these models, this occurs at high energies gaps directly after the highest central density before quark matter appears in the hybrid stars. The region of the MR curves where the slope negative is expected to be an unstable branch of NSs. The stability of branches in the MR curves in the CSS formulation of hybrid stars is expressed in detail by [2].

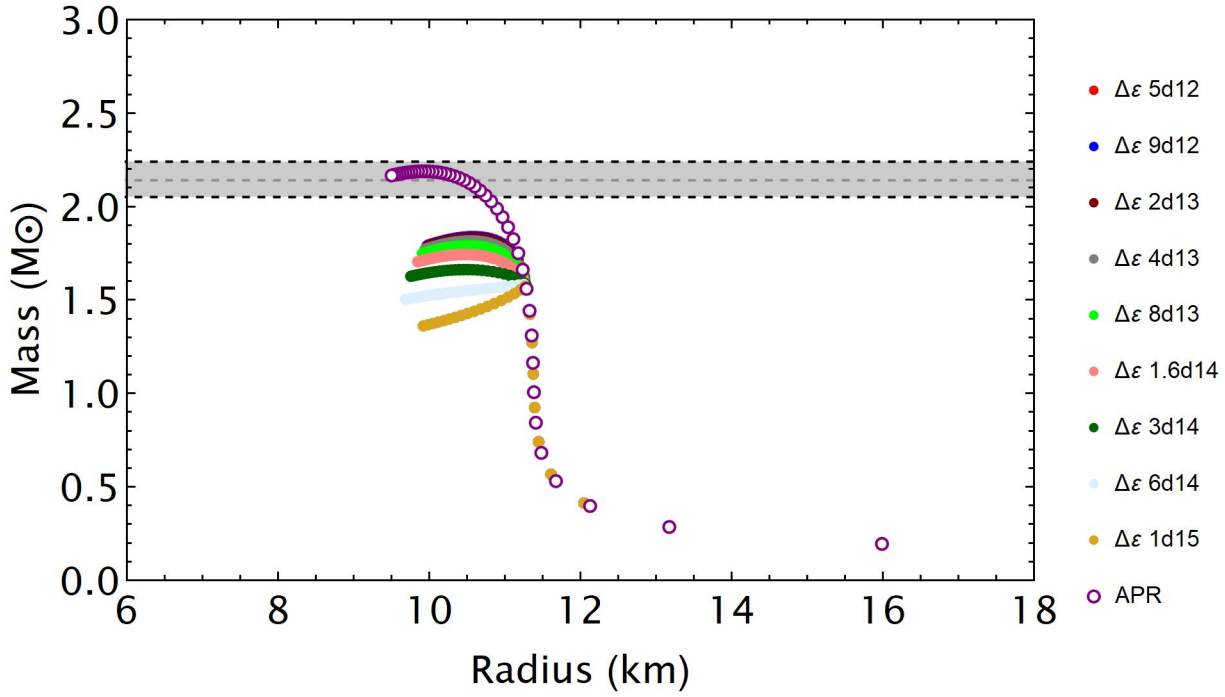

Figure 18: Mass vs. radius relation for hybrid star with the APR nuclear matter EoS with changing energy gap, all with the transition pressure 2×10^{35} dyn cm^{-2}.

At the higher transition pressure, the effects of the energy gaps on the Love-C are less noticeable, but still prevalent. In Figure 19, the larger energy gaps trend to smaller tidal deformations, although even the largest values of the energy gap are similar to the lower bound on the Love-C relation provided by Lattimer [15].

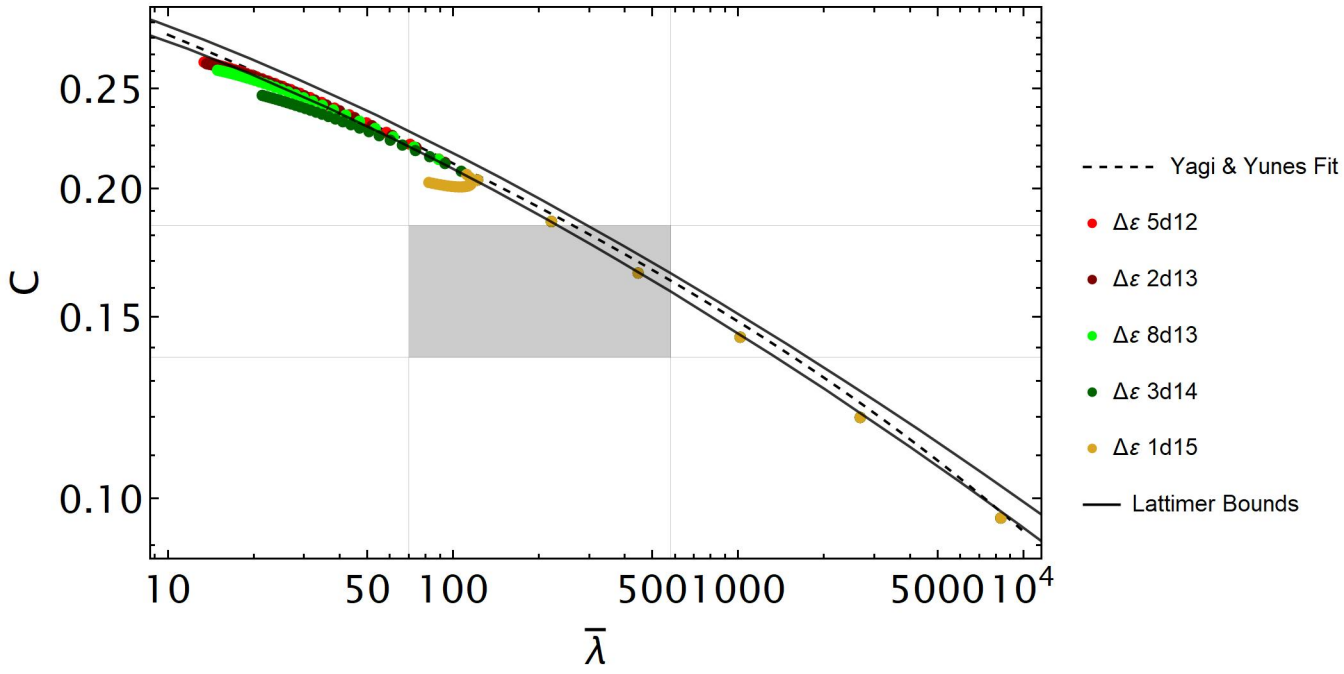

Figure 19: Love-C relation for hybrid star with the APR nuclear matter EoS with changing energy gap, all with the transition pressure 2×10^{35} dyn cm^{-2}.

Again, at the lowest transition pressure of 2×10^{33} dyn cm^{-2}, the effects of changes to the quark matter equation of state are the greatest. The largest masses are seen at the smaller values for energy gap, with larger radii than the fluid APR star. With increasing energy gap, the hybrid star models decrease both in mass and in radius. For the parameter space tested, the hybrid stars' mass-radius curves don't show the same degree of flattening as was seen at higher transition pressure. The Love-C relations of these hybrid star models, seen in Figure 21 show the same trend as the higher transition pressures, although the deviation from the Love-C at the highest energy gaps is smaller than that of the higher 2×10^{34} dyn cm^{-2} transition pressure models, something unexpected as a larger portion of the star is expected to be composed of the solid quark matter at lower transition pressures.

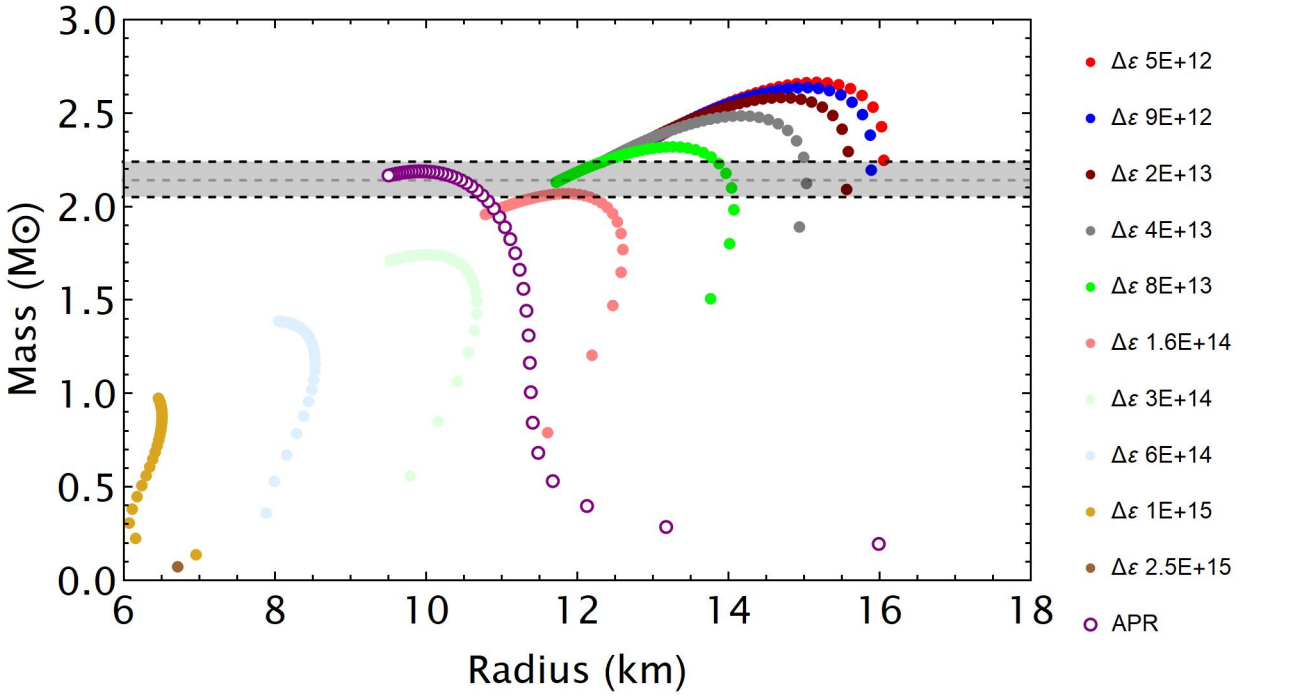

Figure 20: Mass vs. radius relation for hybrid star with the APR nuclear matter EoS with changing energy gap, all with the transition pressure 2×10^{33} dyn cm^{-2}.

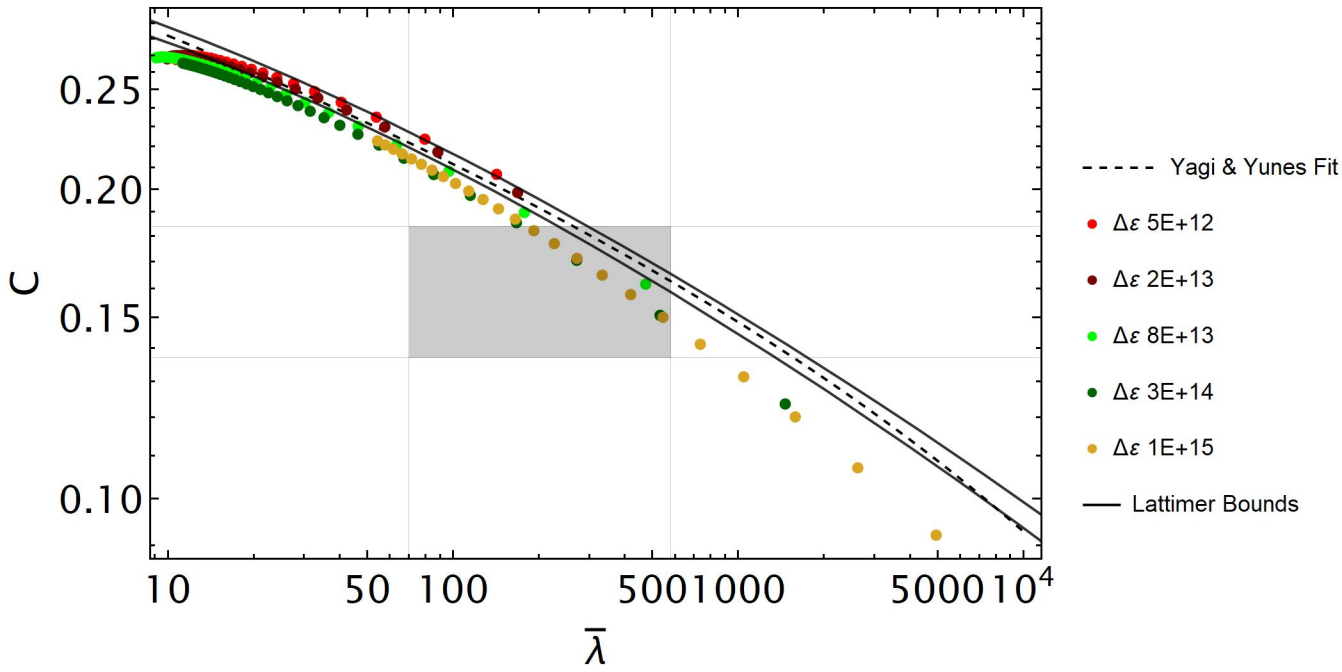

Figure 21: Love-C relations for hybrid star with the APR nuclear matter EoS with changing energy gap, all with the transition pressure 2×10^{33} dyn cm^{-2}.

From this section, modifying the energy gap of the CSS quark matter demonstrates a significant effect on the Love-C relation of hybrid stars. However, the rigidity of these hybrid stars also plays

a direct role in causing deviation from the Love-C universal relation. The numerical code used to perform these calculations outputs the tidal Love number both including and excluding the effects of the rigid core. We can then compare the Love-C relation followed by a model with a large energy gap including this rigidity with the same equation of state excluding the rigidity of the core to separate these two effects. Figure 22 shows a model with a relatively large value calculated at a transition pressure of 2×10^{34} dyn cm^{-2} and a sound speed squared of $\frac{1}{3}$ the speed of light. Love-C calculations for this model both including and excluding the effects of the rigid core are included. Even when excluding the rigidity of the core, there is a significant deviation, indicating that $\Delta\varepsilon$ plays a major role in the Love-C relation of a hybrid model.

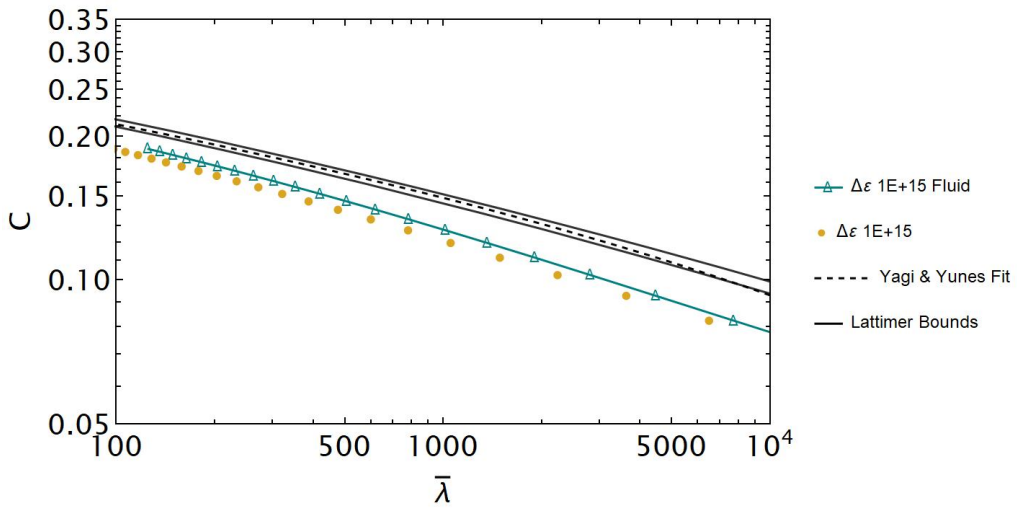

Figure 22: This figures shows the Love-C relation of CSS hybrid star model with the APR nuclear matter envelope with a large value of the $\Delta\varepsilon$. The blue line with open markers shows the Love-C calculations excluding the effects of the crystalline solid core, and the gold, filled markers shows the same model with the solid core effects. While the solid core has a large effect on this calculation, the values excluding the solid show significant deviation from the Love-C universal relation, demonstrating the impact of the energy gap on Love-C.

7 Investigating Deviation of CSS Models Agreeing with Observation

Understanding the effects that the various parameters of the CSS model have on the stellar structure and Love-C universal relations of the hybrid, we can investigate the behavior of multiple nuclear matter envelopes and find regions of parameter space for models that fit the current observational constraints on the masses and radii.

7.1 Comparison of Parameter Space Search to Currently Available Observational Data

The more observations that are made of NSs, especially those in binaries where there are good constraints on the individual masses of the NSs, the better our knowledge is of the mass range of these objects. One of the strongest and most reliable observational constraints that is available

for reducing the parameter space of EoSs is the heaviest measured NS mass. One of the heaviest NSs that have been currently been measured has a mass of $2.14^{+0.10}_{-0.09}M_{\odot}$ [3]. Using techniques based upon relativistic Shapiro delay, this collaboration combined data from the NANOGrav collaboration and recent Green Bank Telescope observations in order to calculate this mass. By requiring the mass-radius curves of the NS reach at least this heavy of a mass at some point, then EoSs that produce lighter hybrid stars can be eliminated.

With recent addition of the NICER telescope to the ranks of the measurement tools of NSs, we are equipped with even more constraints on the EoSs of NSs. By measuring the time variability of hot spots on the spinning NS surface and fitting these emission patterns to models, measurements of the masses and radii have been obtained for NSs. Two pulsars that have been measured via this method, J0740+6620 [22] and J0030+0451[23], provide bounds in the mass-radius space that provide additional constraints on the equations of state.

7.1.1 APR

Continuing the study with APR EoS as the envelope to the hybrid stars in these models, we check at a variety of sound speeds and with changing energy gaps which models agree with the observational constraints on mass and radius.

For four separate sound speeds, a range of energy gaps were plotted against observational constraints to inform a smaller region of parameter space to investigate deviation from Love-C of these hybrid star models. When looking at these MR curves, seen in Figure 23, we are looking for mass-radius curves that go through both of the pulsar constraints, while simultaneously reaching a high enough mass to be consistent with the heaviest measured NS. The observational constraints from LIGO were used less stringently than other observational constraints, as their process for obtaining these values uses universal relations-based methods, something in which deviation is being sought in this investigation. Additionally, in previous sections the effects of large energy gaps on the Love-C relation were found to be significant, thus, parameter space for further investigation for the several sound speeds was also chosen in order to see larger deviation, i.e. the higher end of energy gaps were preferred to be studied in more detail if matching observational constraints.

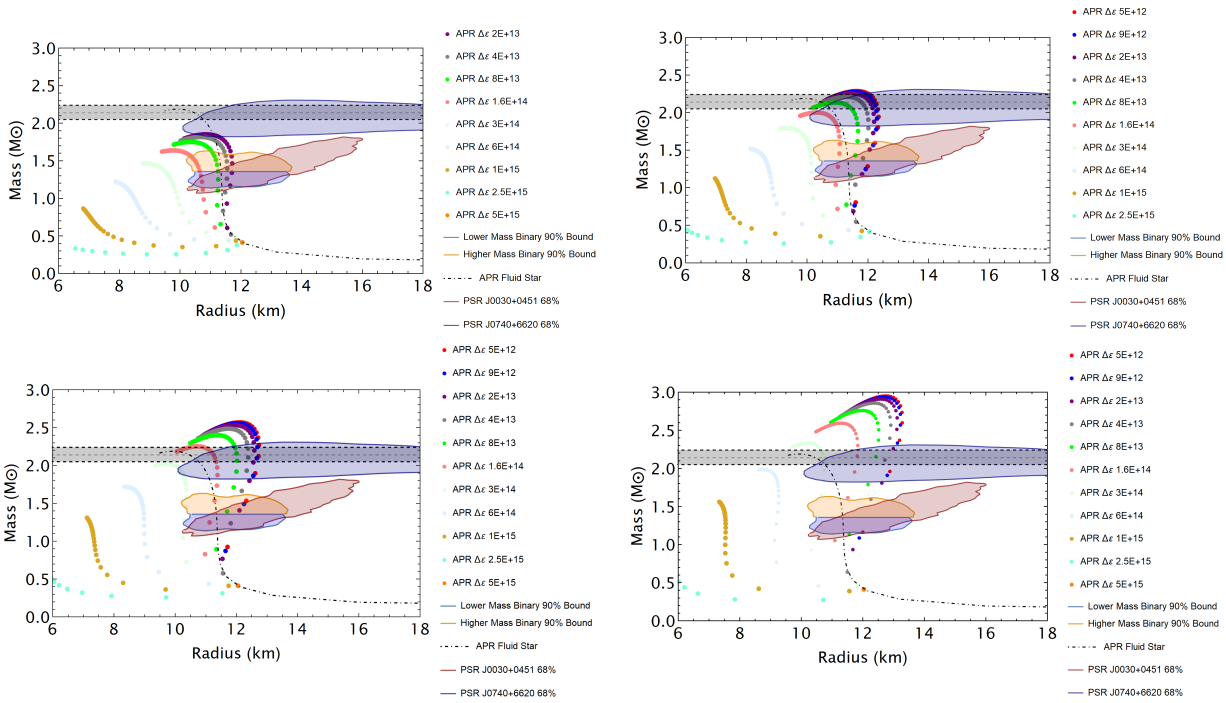

Figure 23: APR Hybrid Star Models with: (Top Left) $c_s^2 = \frac{1}{3}$, (Top Right)$c_s^2 = \frac{1}{2}$, (Bottom Left) $c_s^2 = \frac{2}{3}$, (Bottom Right)$c_s^2 = 1$. Plotted with these Mass-Radius curves are constraints from the observation of NSs from NICER, NANOGrav, and LIGO, [23],[22],[3],[24]. These observations are used in plots throughout this section.

$c_s^2 = \frac{1}{3}$. From the broader parameter space search in Figure 23, APR hybrid star models with a sound speed squared of one-third tended to result in NS masses that are too small compared to the heaviest measured NS [3]. However, some of the models fall within 2 sigma of this NS mass, simultaneously passing through the MR constraints by NICER. The range of $\Delta\varepsilon$ was examined in more detail is from $4 \times 10^{13} - 1.6 \times 10^{14}$ g cm^{-3}. The MR curves for this range are shown in Figure 24.

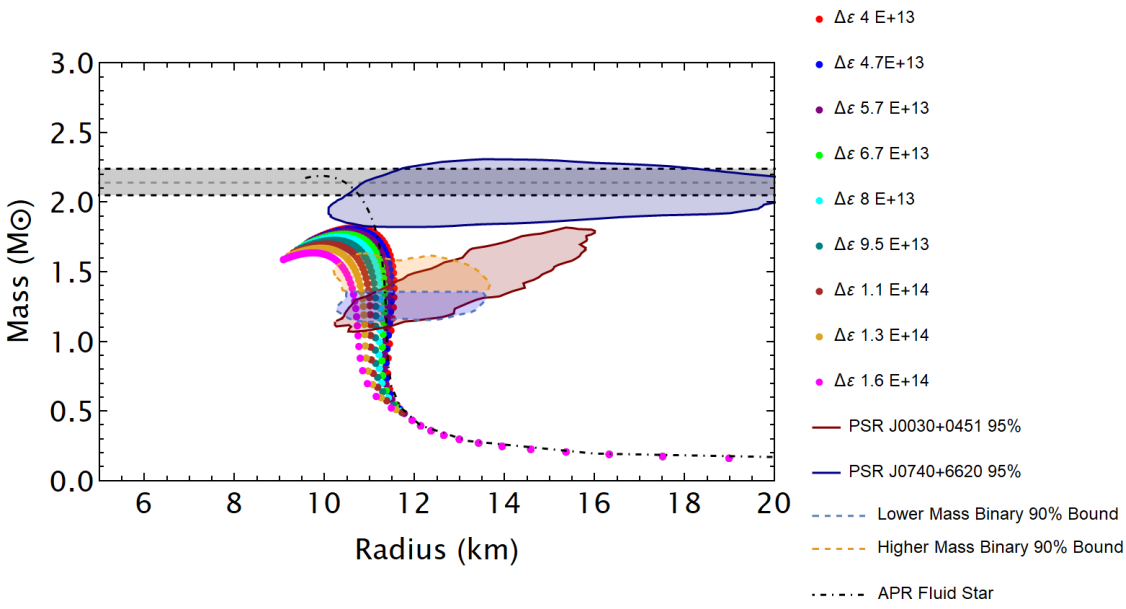

Figure 24: MR relations of APR hybrid star models with $c_s^2 = \frac{1}{3}$ with energy gaps narrowed to match mass-radius observations.

Taking the smallest, intermediate, and largest energy gaps of these hybrid star models, the Love-C relations of this set of models are analyzed in conjunction with the fractional error (Figure 25). All of these models show deviations below 10% level and tend to increase at larger values of tidal deformability.

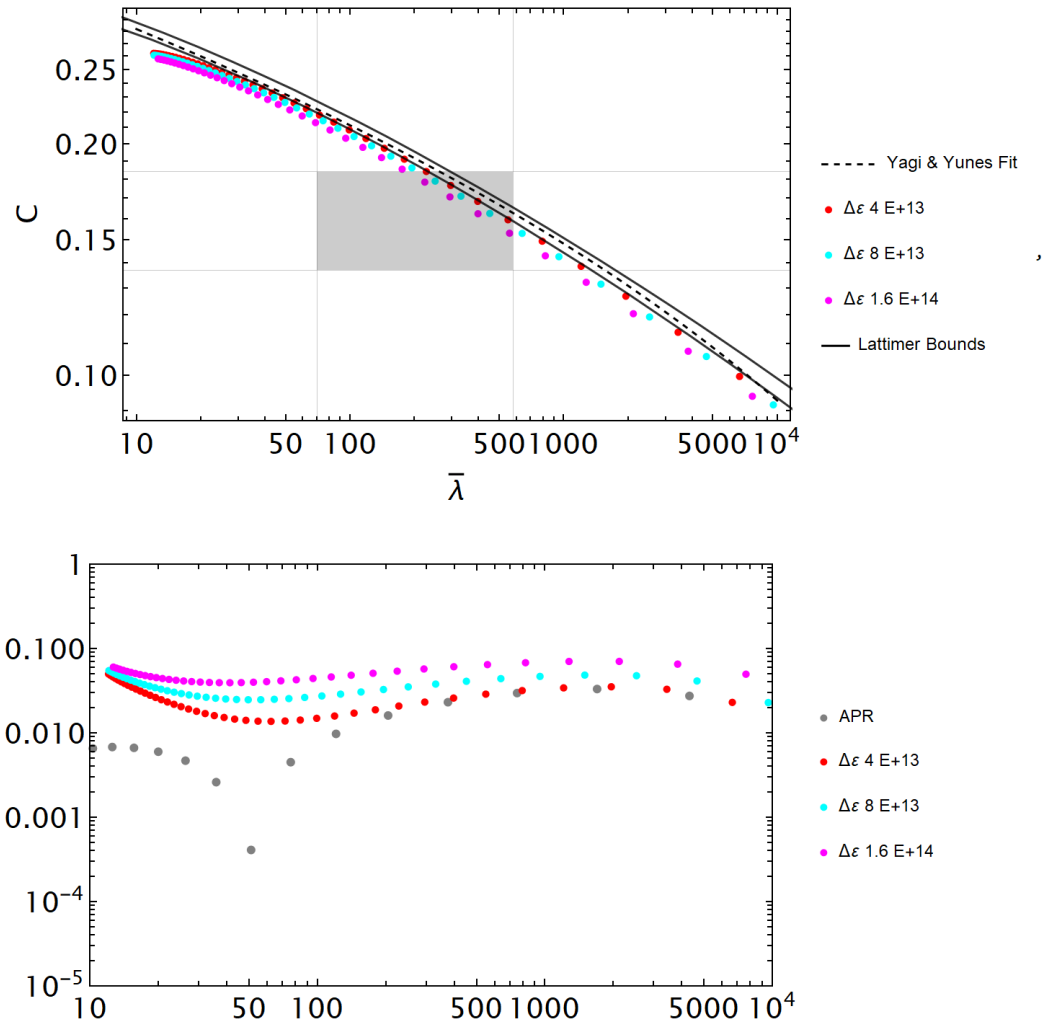

Figure 25: (Top) Love-C relations of APR hybrid star models with $c_s^2 = \frac{1}{3}$ with energy gaps parameters narrowed to match mass-radius observations. (Bottom) Fractional error in the compactness of these models compared to the fluid APR NS fractional error.

$c_s^2 = \frac{1}{2}$. From the broader parameter space search in Figure 23, this set of hybrid stars reaches much larger masses with the increases in stiffness. The range of $\Delta\varepsilon$ that was examined in more detail, based upon the adherence to observational constraints with potentially large deviations from Love-C, is from $4 \times 10^{13} - 1.6 \times 10^{14}$ g cm^{-3}. The MR curves for this range are shown in Figure 26.

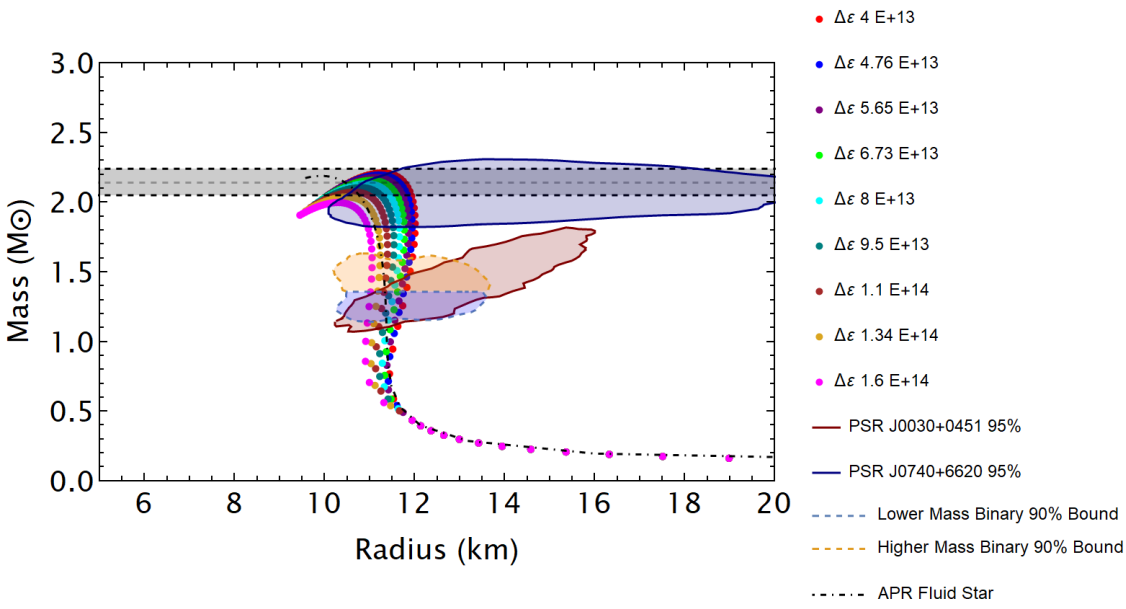

Figure 26: MR relations of APR hybrid star models with $c_s^2 = \frac{1}{2}$ with energy gaps narrowed to match mass-radius observations.

The Love-C relations of this set of models were plotted for three values of this energy gap, found in Figure 27. These models show lower levels of fractional error compared to the previous set of $\frac{1}{3}$ sound speed squared hybrid star models. The deviation tended to be smaller at the lower values of the tidal deformability and increase with the increased levels of tidal deformability. The places in the fractional error plot where the relations seem to diverge represent the crossing of the Love-C relation of the model with the best-fit line to the Love-C universal relation.

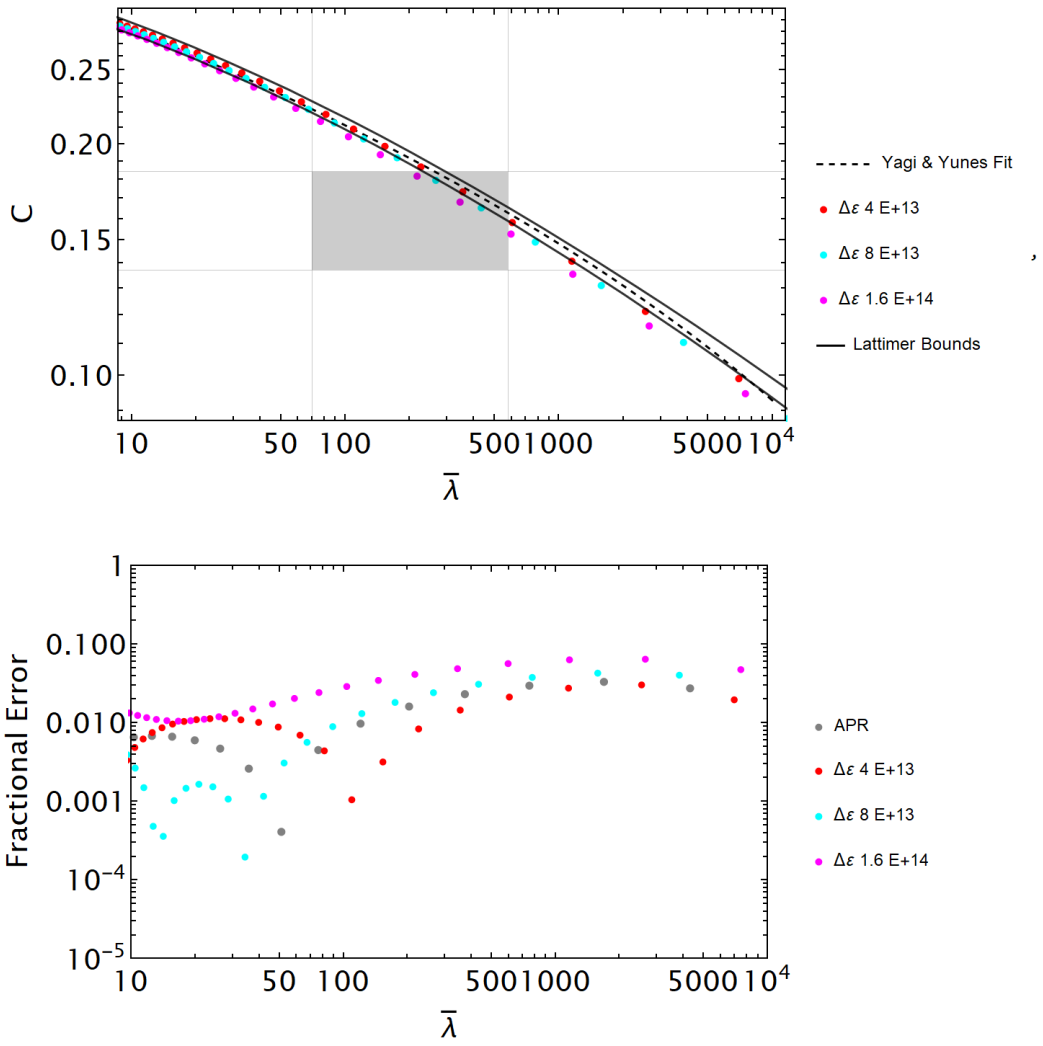

Figure 27: (Top) Love-C relations of APR hybrid star models with $c_s^2 = \frac{1}{2}$ with energy gaps parameters narrowed to match mass-radius observations. (Bottom) Fractional error in the compactness of these models compared to the fluid APR NS fractional error.

$c_s^2 = \frac{2}{3}$. In the bottom left of Figure 23, there is a wide range of masses and radii covered by the set of changing energy gap parameters to the CSS hybrid stars models. The increase in stiffness of the equation of state as compared to the previous set of models means that larger stars can be supported, and larger energy gap values can be used in the models while still producing massive enough stars. The increase in energy gap tends to decrease the masses and radii of the hybrid stars in this model, yet increases the deviation from the Love-C relation. Thus, the stiffer hybrid star equations of state may be a prime location to constrain hybrid star equations of state. The range of $\Delta\varepsilon$ that was examined in more detail is from $2 \times 10^{13} - 3 \times 10^{14}$ g cm^{-3}. The MR curves for this range are shown in Figure 28.

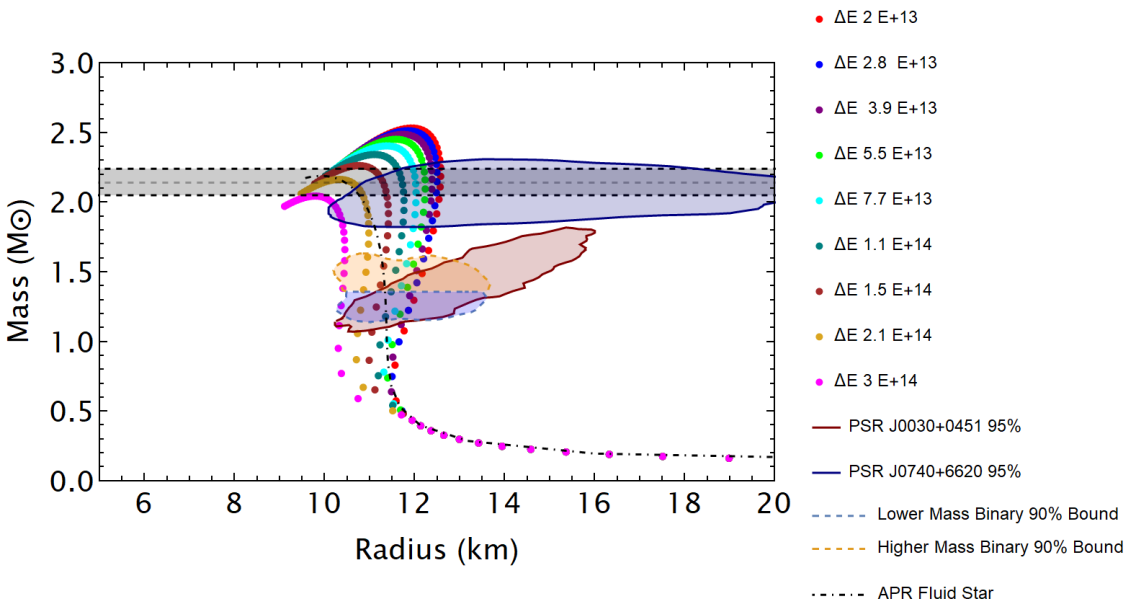

Figure 28: MR relations of APR hybrid star models with $c_s^2 = \frac{2}{3}$ with energy gaps narrowed to match mass-radius observations.

The Love-C relation of these hybrid stars tends (Figure 29 to agree very strongly with the universal relation at the low tidal deformabilities, but saw an increase in the fractional error at higher values of tidal deformability. For the most extreme energy gap of 3×10^{14} g cm^{-3}, the deviations from the best fit were larger than 10%, while still passing through the edge regions of the constraints provided by the NICER pulsars. This shows that models with large stiffness, increasing their ability to reach massive enough stars, and large energy gaps, which are shown to have a strong effect on the tidal deformability of NSs, provide an interesting region of parameter space to explore for constraining the dense matter equation of state.

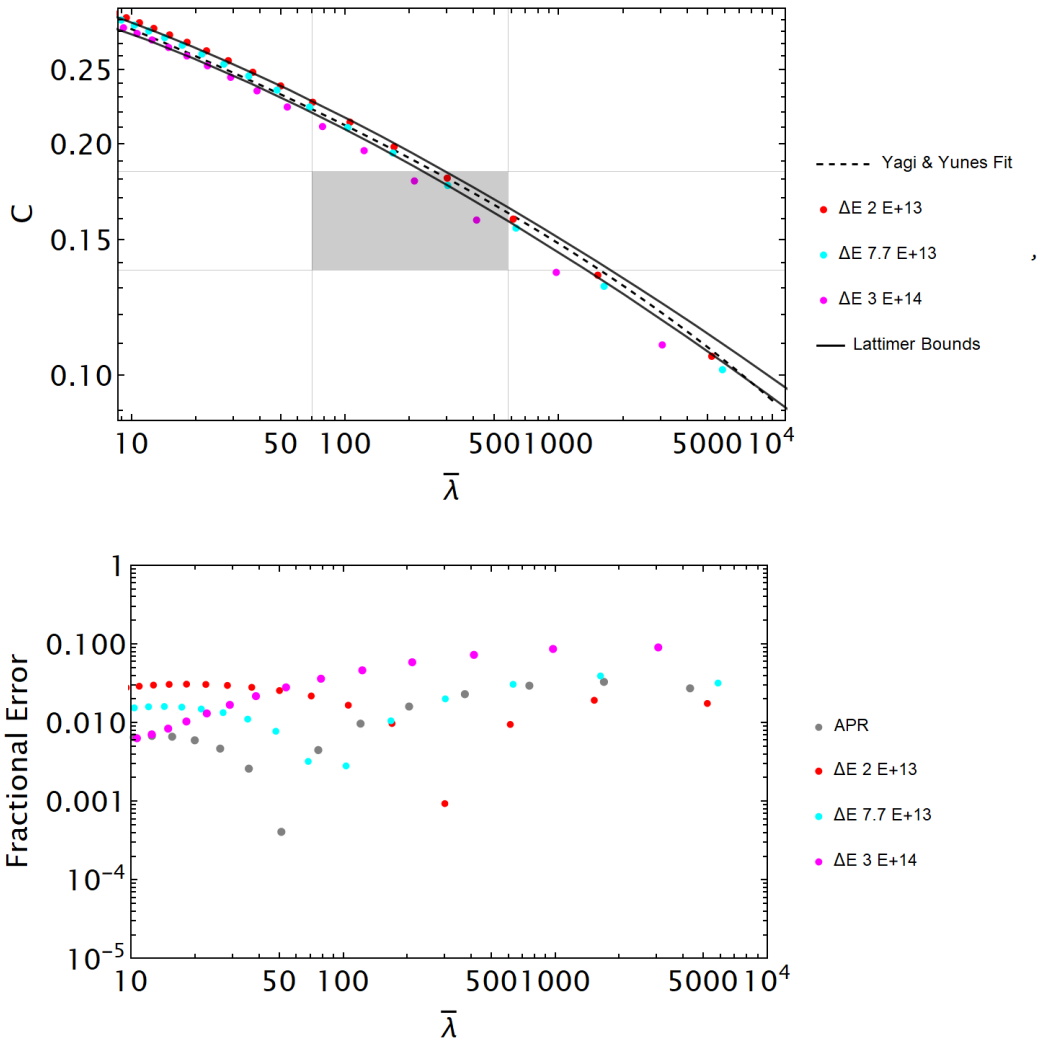

Figure 29: (Top) Love-C relations of APR hybrid star models with $c_s^2 = \frac{2}{3}$ with energy gaps parameters narrowed to match mass-radius observations. (Bottom) Fractional error in the compactness of these models compared to the fluid APR NS fractional error.

$c_s^2 = 1$. The highest sound speed considered in this broad sweep of parameters was a sound speed squared equal to the causal limit, the speed of light squared (in natural units, 1). While this is likely a nonphysical compact object, it presents an interesting case to consider for the constant sound speed hybrid star models that are equipped with this interior rigidity. The large stiffness of the hybrid star models with this central sound speed enables models to reach the higher masses with more extreme values of the energy gap parameter $\Delta\varepsilon$. Based on the observational constraints on the mass-radius, the range of $\Delta\varepsilon$ that was chosen is $2 \times 10^{13} - 3 \times 10^{14}$ g cm^{-3}. The MR curves for this range are shown in Figure 30. The maximum masses of this set of hybrid star models have a maximum mass of just under $3M_\odot$ for the lowest value of $\Delta\varepsilon$.

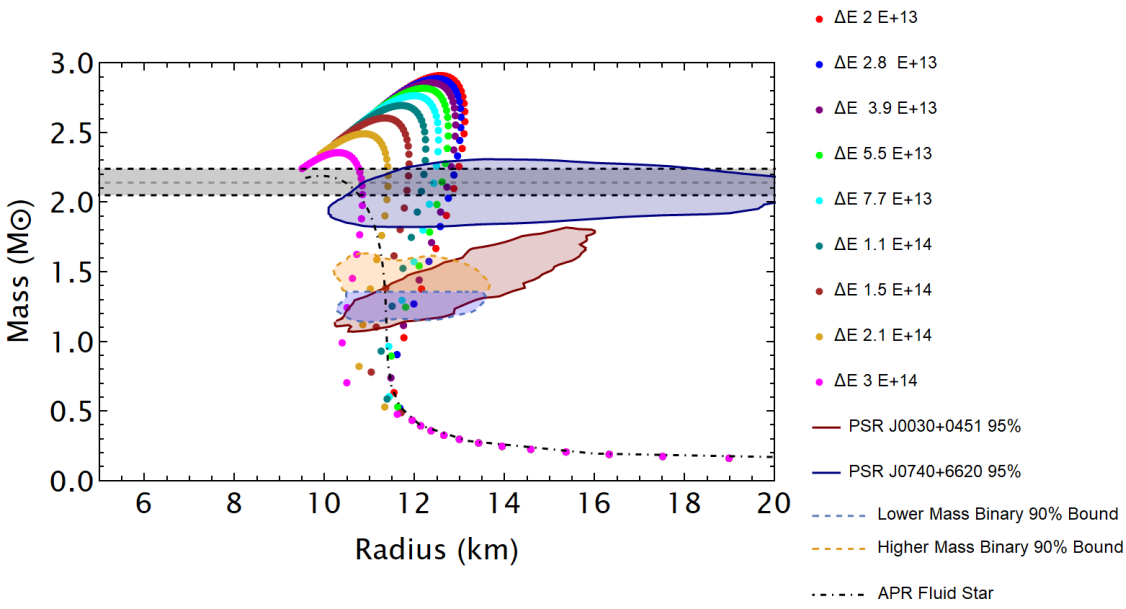

Figure 30: MR relations of APR hybrid star models with $c_s^2 = 1$ with energy gaps narrowed to match mass-radius observations.

When comparing the Love-C relations of the lowest, middle, and highest energy gap considered in Figure 31, again there are models that fit the mass-radius constraints with deviations from the Love-C universal relation upward of 10%. While these models are less physical, they show that there is a range of parameters within the CSS framework of nuclear matter-quark matter hybrid stars that do not agree with the universal relations.

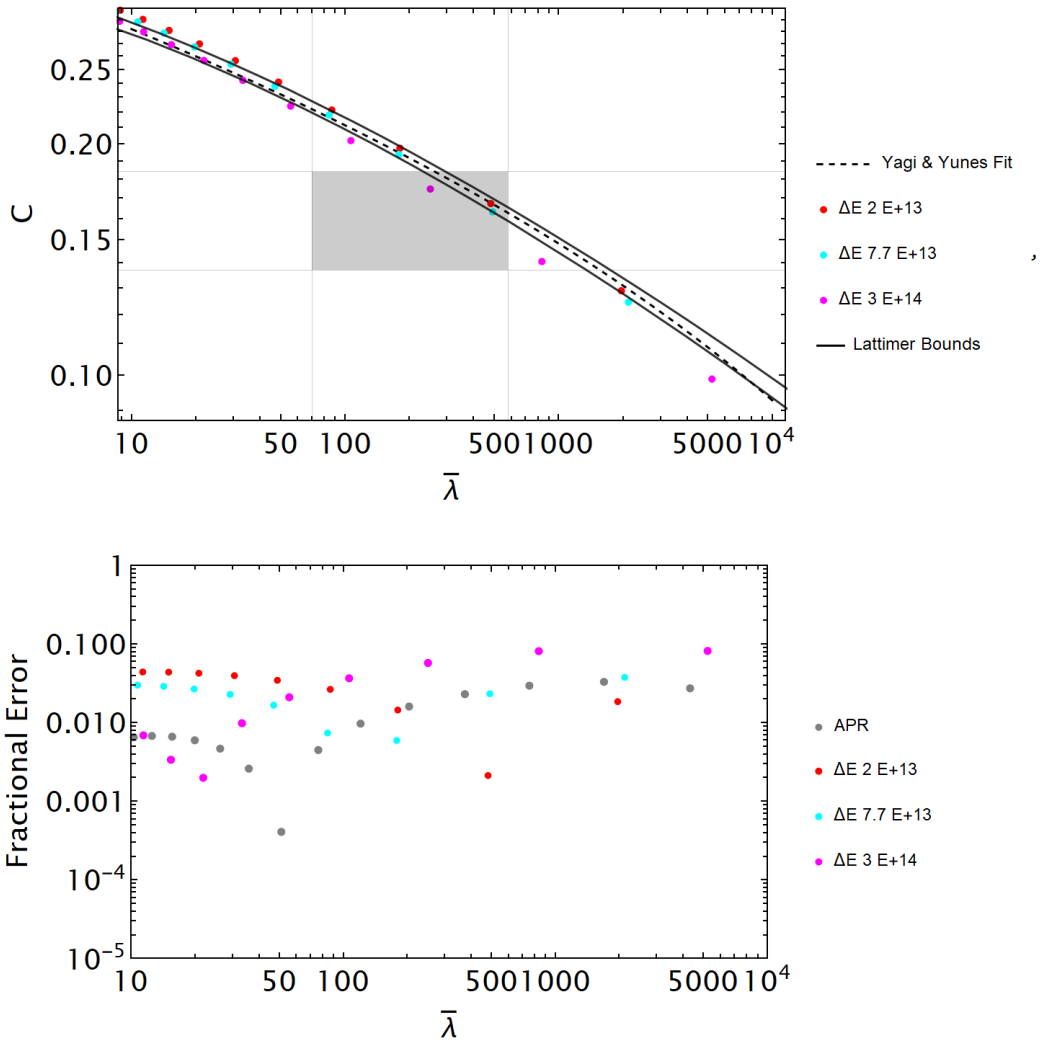

Figure 31: (Top) Love-C relations of APR hybrid star models with $c_s^2 = 1$ with energy gaps parameters narrowed to match mass-radius observations. (Bottom) Fractional error in the compactness of these models compared to the fluid APR NS fractional error.

7.1.2 SLy4

Further investigation into the parameter space of the CSS Models with SLy4 nuclear matter represented in Figure 23 will be considered in future projects.

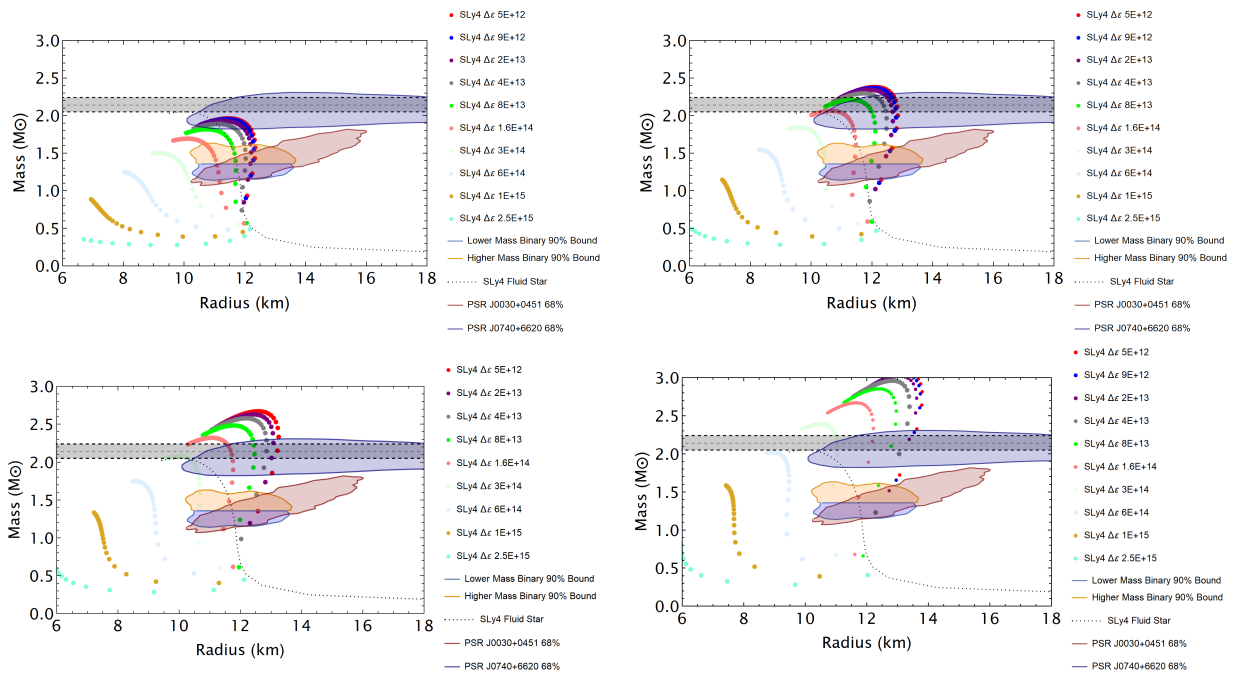

Figure 32: Hybrid Star Models with: (Top Left) $c_s^2 = \frac{1}{3}$, (Top Right) $c_s^2 = \frac{1}{2}$, (Bottom Left) $c_s^2 = \frac{2}{3}$, (Bottom Right) $c_s^2 = 1$. Plotted with these mass-radius curves are constraints from the observation of NSs from NICER, NANOGrav, and LIGO

7.1.3 NL3

Further investigation into the parameter space of the CSS Models with NL3 nuclear matter envelopes represented in Figure 23 will be considered in future projects.

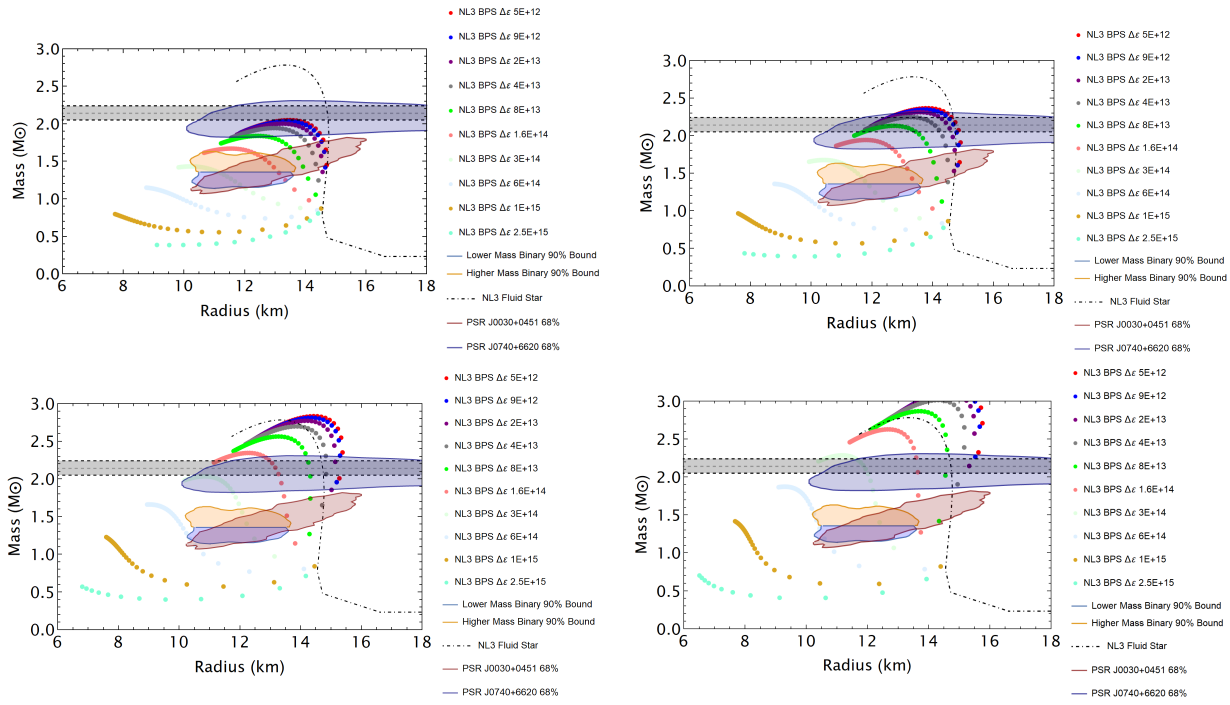

Figure 33: NL3 Hybrid Star Models with: (Top Left) $c_s^2 = \frac{1}{4}$, (Top Right)$c_s^2 = \frac{1}{3}$, (Bottom Left) $c_s^2 = \frac{1}{2}$, (Bottom Right)$c_s^2 = \frac{2}{3}$. Plotted with these Mass-Radius curves are constraints from the observation of NSs from NICER, NANOGrav, and LIGO

8 Conclusions & Future Work

The nature of the dense matter equation of state remains an open question, as physicists from a variety of disciplines attempt to tackle these questions from different perspectives. The advent of multi-messenger astronomy presents a unique opportunity for constraining the vast set of models that try to describe the behavior of matter at the extremely high densities characteristic of NS cores, as observations of mass, radius, and values of NS tidal deformability are obtained from measurements. The combination of cutting-edge gravitational wave measurements, X-ray telescopes, and radio astronomy observations provide stronger constraints on the properties of NSs that need to be met by any theoretical prediction of the dense matter equation of state.

Given a specific equation of state, the TOV equations can then be solved under initial conditions to yield predictions of the mass and radius of an NS. Additionally, under the general relativistic formalism that describes the appropriate NS, the tidal deformability of the specific NS can be calculated as a perturbation to a background, perfect-fluid solution to the TOV equations. The specific phase of dense matter that we investigated in this study was the CCS phase of deconfined quark matter, a possible candidate phase of matter in the low-temperature and high-density regimes. This quark matter phase involves the pairing of deconfined quarks through a process called LOFF pairing [1],[17], which allows the quark matter to form a crystalline structure with a significant shear modulus, a property that would be expected to have a relevant impact on the tidal Love number of the NS. We conducted calculations for both mass-radius curves and the tidal deformability of hybrid NSs with CCS quark matter cores, incorporating first by an MIT Bag Model type formulation and second by a constant sound speed model [2] coupled with a density-based shear modulus, developed during this investigation.

Using the CSS parameterization of the CCS quark matter hybrid stars, there were a variety of trends that could be seen in the MR and Love-C relations. When the transition from nucelar matter to quark matter occurred at lower pressures, the model hybrid star was made up of a larger percentage of quark matter. This tended to amplify the effects that the stiffness and energy gap had on these relations. Increasing the sound speed affected the MR curves as expected, producing NS of heavier masses, while shifting the Love-C relations of these stars toward higher deformabilities and higher compactness values for the same central density. Increasing the energy gap showed significant effects on both MR and Love-C. Higher values of $\Delta\varepsilon$ tended to flatten the mass-radius curves, even causing positive values of $\frac{dM}{dR}$, which are unstable NS branches as described by [2]. Additionally, the larger values of energy gap caused significant deviation from Love-C, shifting the relation toward smaller tidal deformabilities.

We found various models in the parameter space of the CSS formulation that 1) agree with the observational constraints on the masses and radii of NS and 2) demonstrate deviation from the Love-C universal 10% or greater. The portions of the parameter space with large deviations from Love-C exhibit represent interesting cases with which we may be able further to constrain the properties of possible CCS hybrid stars. Especially with longer observing runs of gravitational wave observatories like LIGO and the increase in their sensitivity, there hopes to be more measurements of the tidal Love number with smaller bounds on this value, which will further the ability to make constraints based on the Love-C universal relation.

8.1 Future Work

While the nuclear matter envelope EoS used primarily throughout this study was the APR [13] EoS, this work was also conducted with Sly4 and NL3 equations of state, which have different degrees of stiffness and predictions for the mass-radius of NSs. Further investigation into the parameter space with these nuclear matter envelopes may shed more light on the behavior of the CCS hybrid stars, further probing the dense matter equation of state. Additionally, a majority of the parameter space search was conducted at the nominal transition pressure; however, the lower transition pressure shows very interesting stellar structure and Love-C relations that are not all strictly forbidden based on current mass-radius constraints.

9 Acknowledgements

This thesis would not have been possible without the guidance of **Prof. Kent Yagi** of the University of Virginia. His guidance and direction throughout this project were invaluable, and this process has allowed me to grow as a researcher and scientist. I am very grateful for his mentoring throughout this project. The gravity group at UVA is wonderful, and they have been a point of constant support and wisdom.

Additionally, this project would not have occurred without the help of **Shu Yan Lau**. He is the original author of the numerical code for the TOV and relativistic tidal deformability calculations that was used throughout this experiment. He has been incredibly helpful and supportive throughout the entire research. I am very thankful for his constant positivity and patience which have made this process possible.

Lastly, the support from my peers has been essential for my success. The following people have made this process possible: UVA Astrophysics fourth-year students Ethan McKeever, Louis Seyfritz, Jee-Ho Kim, Theo O'Neill, Sarah Shriner, Mint Tositrakul, Alex Palaoro, and Jillian

Maxson. UVA Physics fourth-year students Jason Boynewicz, Sophia Yi, Philip Velie, and Darren Upton. Chemistry students Sarah Lombardo, Rachel Lombardo and Andrew DiSanto.

References

[1] A. I. Larkin and Y. N. Ovchinnikov, Zh. Eksp. Teor. Fiz. **47**, 1136 (1964).

[2] M. G. Alford, S. Han, and M. Prakash, Physical Review D **88**, 10 . 1103 / physrevd.88.083013 (2013).

[3] H. T. Cromartie, E. Fonseca, S. M. Ransom, P. B. Demorest, Z. Arzoumanian, H. Blumer, P. R. Brook, M. E. DeCesar, T. Dolch, J. A. Ellis, R. D. Ferdman, E. C. Ferrara, N. Garver-Daniels, P. A. Gentile, M. L. Jones, M. T. Lam, D. R. Lorimer, R. S. Lynch, M. A. McLaughlin, C. Ng, D. J. Nice, T. T. Pennucci, R. Spiewak, I. H. Stairs, K. Stovall, J. K. Swiggum, and W. W. Zhu, Nature Astronomy **4**, 72 (2019).

[4] S. Bogdanov, F. K. Lamb, S. Mahmoodifar, M. C. Miller, S. M. Morsink, T. E. Riley, T. E. Strohmayer, A. K. Tung, A. L. Watts, A. J. Dittmann, D. Chakrabarty, S. Guillot, Z. Arzoumanian, and K. C. Gendreau, The Astrophysical Journal Letters **887**, L26 (2019).

[5] M. Alford, J. A. Bowers, and K. Rajagopal, Physical Review D **63**, 10.1103/physrevd.63.074016 (2001).

[6] K. Yagi and N. Yunes, Physics Reports **681**, 1 (2017).

[7] K. Yagi and N. Yunes, Science **341**, 365 (2013).

[8] A. Maselli, V. Cardoso, V. Ferrari, L. Gualtieri, and P. Pani, Phys. Rev. D **88**, 023007 (2013).

[9] S. Y. Lau, P. T. Leung, and L.-M. Lin, Phys. Rev. D **99**, 023018 (2019).

[10] K. S. Thorne, Phys. Rev. D **58**, 124031 (1998).

[11] T. Hinderer, The Astrophysical Journal **677**, 1216 (2008).

[12] G. Shen, C. J. Horowitz, and S. Teige, Physical Review C **83**, 10 . 1103 / physrevc.83.035802 (2011).

[13] A. S. Schneider, C. Constantinou, B. Muccioli, and M. Prakash, Physical Review C **100**, 10 . 1103 / physrevc . 100 . 025803 (2019).

[14] Douchin, F. and Haensel, P., A&A **380**, 151 (2001).

[15] S. Postnikov, M. Prakash, and J. M. Lattimer, Phys. Rev. D **82**, 024016 (2010).

[16] M. Alford, M. Braby, M. Paris, and S. Reddy, The Astrophysical Journal **629**, 969 (2005).

[17] P. Fulde and R. A. Ferrell, Phys. Rev. **135**, A550 (1964).

[18] M. Mannarelli, K. Rajagopal, and R. Sharma, Phys. Rev. D **76**, 074026 (2007).

[19] B. P. Abbott et al. (The LIGO Scientific Collaboration and the Virgo Collaboration), Phys. Rev. Lett. **121**, 161101 (2018).

[20] H. O. Silva, A. M. Holgado, A. Cárdenas-Avendaño, and N. Yunes, Phys. Rev. Lett. **126**, 181101 (2021).

[21] A. Kurkela, P. Romatschke, A. Vuorinen, and B. Wu, *Looking inside neutron stars: microscopic calculations confront observations*, 2010.

[22] M. C. Miller, F. K. Lamb, A. J. Dittmann, S. Bogdanov, Z. Arzoumanian, K. C. Gendreau, S. Guillot, W. C. G. Ho, J. M. Lattimer, M. Loewenstein, S. M. Morsink, P. S. Ray, M. T. Wolff, C. L. Baker, T. Cazeau, S. Manthripragada, C. B. Markwardt, T. Okajima, S. Pollard, I. Cognard, H. T. Cromartie, E. Fonseca, L. Guillemot, M. Kerr, A. Parthasarathy, T. T. Pennucci, S. Ransom, and I. Stairs, The Astrophysical Journal Letters **918**, L28 (2021).

[23] M. C. Miller, F. K. Lamb, A. J. Dittmann, S. Bogdanov, Z. Arzoumanian, K. C. Gendreau, S. Guillot, A. K. Harding, W. C. G. Ho, J. M. Lattimer, R. M. Ludlam, S. Mahmoodifar, S. M. Morsink, P. S. Ray, T. E. Strohmayer, K. S. Wood, T. Enoto, R. Foster, T. Okajima, G. Prigozhin, and

Y. Soong, The Astrophysical Journal **887**, L24 (2019).

[24] B. Abbott et al., Physical Review Letters **121**, 10.1103/physrevlett.121.161101 (2018).